Stemflow and Stemflow Infiltration Area for Isolated Ponderosa Pine in a Semi-Arid Setting

By

Brandon Michael Makar

B.A., Thompson Rivers University, 2020

A Thesis Submitted in Partial Fulfillment of the Requirements for the Degree of Master of Science in Environmental Sciences

in the Faculty of Science

Thompson Rivers University

Kamloops, British Columbia, Canada

July 2026

Thesis Examining Committee:

Dr**.** Darryl Carlyle-Moses (PhD), Thesis Co-Supervisor and Professor, Department of Environment, Culture and Society, Thompson Rivers University

Dr. Tom Pypker (PhD), Thesis Co-Supervisor, Professor and Chair, Department of Natural Resource Sciences, Thompson Rivers University

Dr. Wendy Gardner (PhD), Committee Member, Professor, Department of Natural Resource Sciences, Thompson Rivers University

Dr. Delphis Levia (PhD), External Examiner, Professor, Department of Geography and Spatial Sciences, University of Delaware

Abstract

Stemflow and stemflow infiltration into soil is of hydrological, geomorphological, and biogeochemical importance. I studied stemflow in twelve isolated ponderosa pine trees in a semi-arid environment characterized by both short, intense storms and long, less intense storms. To determine the effects of meteorological variables upon stemflow volumes, percent, and funneling ratios, I included rainfall depth, rainfall inclination angle, rainfall duration, rainfall intensity, wind speed, and evaporation. Stemflow had an overwhelming relationship with rainfall depth, and was also affected by rainfall inclination, duration, and in some cases evaporation. To determine the effects of tree morphological variables upon stemflow volumes, percent, and funnelling ratio, I analysed bark relief index, branching angle, canopy height, canopy height to width ratio, canopy volume, diameter at breast height, projected canopy area, and tree height. Small diameter trees with high branching angles tended to produce higher stemflow at lower thresholds, while large diameter trees with high branching angles tended to produce maximum stemflow amounts. To determine the effects of stemflow flow rates and tree morphology on the stemflow infiltration area, I simulated rates given by my twelve trees and measured the extent of the infiltration area. Due to the taproot nature of ponderosa pine as well as comparatively low flow, stemflow infiltration area around studied ponderosa pine trees was very small, averaging at 300 cm^2. My results may be used in forest management practices to better preserve the health of ecosystems where applicable. If foresters take into account tree morphological variables outlined in this study, they may be able to better select which trees should be logged and which trees should be left for overall ecosystem health.

Keywords: stemflow, stemflow infiltration area, branch angles, ponderosa pine, semi-arid, forest hydrology, rainfall inclination angle, funnelling ratio

Table of Contents

Acknowledgements

I would like to thank the following people for their unwavering support during the course of my master's degree:

- Dr. Darryl Carlyle-Moses and Dr. Tom Pypker, my supervisors;
- Adria Huser, my invaluable research assistant;
- Dr. Wendy Gardner, the other member of my supervisory committee;
- Dr. Del Levia, my external examiner;
- TRU Faculty members Crystal Huscroft, Dr. David Hill, Dr. Kim Naqvi, Dr. Michael Mehta, without whom I would not have a bachelor's degree;
- Thompson Rivers University, for allowing us to conduct our research on their property;
- TRU Student Union, for granting me the money to present my research at a conference in Denver, CO;
- My parents, Matt and Monica, and my brother Tyler for joining me on very wet research days;
- My friends and family, who I am sure would be happy to never hear the word "stemflow" again.

All of the above people/entities deserve recognition, as without them I would not be completing this degree. I hope to continue working in environmental science and bring some of the results and recommendations in this thesis to a wider audience

List of Figures

List of Tables

Glossary of Terms

A_B ---------- Branching Angle

B_A ---------- Basal Area

B_n ---------- Number of Branches

B_{RI} ---------- Bark Relief Index

C_H ---------- Canopy Height

C_W ---------- Canopy Width

C_V ---------- Canopy Volume

D_B ---------- Intra-storm Break Duration

D_{BH} ---------- Diameter at Breast Height

D_E ---------- Event Duration

D_R ---------- Rainfall Duration

E ---------- Evaporation Coefficient

F ---------- Funnelling Ratio

H ---------- Tree Height

$I_{max\text{-}5}$ ---------- Maximum 5-min Rainfall Intensity

$I_{wt\text{-}5}$ ---------- Weighted 5-min Rainfall Intensity

I_t ---------- Stemflow Infiltration Area

K_{sat} ---------- Saturated Hydraulic Conductivity

P_{CA} ---------- Projected Canopy Area

P_g ---------- Gross Precipitation Amount

P_g'' ---------- Precipitation Required to Initiate Stemflow

P_{inc} ---------- Precipitation Inclination

Q_{SF} ---------- Stemflow Flow Rate

$R_{H\text{-}W}$ ---------- Canopy Height to Width Ratio

S_F ---------- Stemflow

$S_{F\,\%}$ ---------- Percentage of Rainfall Partitioned into Stemflow

S_{Fr} ---------- During Event Stemflow Flow Rates

T_F ---------- Throughfall

$u_{a,wt-5}$ ---------- Weighted 5-min Wind Speed

V_{PD} ---------- Vapour Pressure Deficit

Chapter 1: Stemflow within a Broader Context

1.1 Understanding Stemflow

Precipitation into forest canopies is divided into three hydrological processes: throughfall (T_F), stemflow (S_F), and canopy interception loss. Throughfall refers to precipitation that makes it through the vegetation canopy (Carlyle-Moses, 2004). Stemflow is the movement of canopy-intercepted water along branches and down the boles of trees and stems of other plants to the ground, sometimes contributing to runoff or infiltrating into the soil. This water mobilizes nutrients, organic matter, and other substances from the plant surfaces as it descends (Whitford et al. 1997; Muoghalu 2003; Wagner et al. 2019). Stemflow is often studied in forest ecosystems to better understand water flow and nutrient distribution within these environments. Historically, S_F's contribution to individual trees has been overlooked because it is volumetrically insignificant at the forest stand or watershed scale relative to T_F's volume (Levia and Frost 2003; Zuecco et al. 2025). Some stemflow studies were present in older literature, but investigations are becoming much more common, owing to the recognition of S_F's ecohydrological significance (e.g. Herwitz 1987; Tanaka 2011; Levia and Germer 2015, Katul et al. 2025, Levia et al. 2025). As S_F is a point-source input of water into soil, it plays a key role in soil hydrology and geochemistry (Schooling and Carlyle-Moses 2015). Despite this, S_F remains under-investigated relative to other tree-water dynamics.

Stemflow is a pivotal component of the hydrological cycle because it can contribute greatly to groundwater recharge and nutrient cycling within ecosystems (Spencer and van Meerveld, 2016; Pinos et al. 2023; de Lima et al. 2026). It is a major pathway for water transfer in forest ecosystems, redistributing precipitation inputs and affecting soil moisture regimes (Durocher 1990). Stemflow conveys nutrients and organic matter from the canopy to the forest floor, thereby enhancing nutrient cycling and soil fertility (Wu et al. 2024). The concentrated nutrient input via S_F drives microbial activity, fosters plant growth, and affects soil biogeochemical processes (Parker 1983; Levia and Frost 2003; Staelens 2007; Wagner, 2019). Certain tree species produce higher rates of stemflow, leading to localized nutrient enrichment and creating favorable conditions for associated flora and fauna (Andersson

1991; Herwitz 1991; Chang 2000; Kuraji 2001). Because S_F is a point-source input to soil, studies have indicated its important role in groundwater recharge (e.g. Tanaka et al. 1996; Germer 2013; Spencer and van Meerveld 2016; Pinos et al. 2023).

1.2 Meteorological Conditions Influencing Stemflow

S_F has been associated with several meteorological conditions, notably that S_F production increases with increasing precipitation (Brown and Barker 1970, Xiao et al. 2000, Staelens et al. 2008; Germer et al. 2010; Van Stan et al. 2014). In some cases, S_F has been found to increase with increasing rainfall intensity after reaching the required threshold for production (Aboal et al. 1999; Van Stan et al. 2014), while in other cases, it decreases (Levia and Frost 2003; Carlyle-Moses 2004; Carlyle Moses and Price 2006; Zabret et al. 2018). The increase in S_F with rainfall intensity has been attributed to trees rapidly reaching the saturation level required to initiate stemflow ($P_g^{''}$) (Aboal et al. 1999). In Van Stan et al. (2014), the correlation between rainfall intensity and S_F was strengthened where larger trees, being the most exposed to storm conditions, increased stemflow production during storms. In some cases, the S_F increase during increasing rainfall intensity has been attributed to the increase in speed and change in direction of wind (e.g Van Stan et al 2011). However, in studies where rainfall intensity has a negative relationship with S_F, reduced stemflow is attributed to rainfall intensity causing larger rain drops, higher drop terminal velocity and kinetic energy (Guo et al. 2022). This results in raindrops splashing off the canopy surface, or stemflow dripping off branches, becoming another form of throughfall rather than stemflow (Price and Carlyle-Moses 2004; Carlyle-Moses 2004; Levia et al. 2010). In addition, S_F has been found to be strongly positively influenced by wind speed, and, perhaps most critically, increasing wind speed lowers the precipitation threshold required for trees to generate stemflow (Levia and Frost 2003; Carlyle-Moses and Price 2007; Carlyle-Moses and Schooling 2015; Zabret et al. 2018). Raindrop size and rainfall inclination angle, which are functions of both wind speed and rainfall intensity, have been shown to positively influence S_F production through the interaction between tree morphology and rainfall inclination angle (Carlyle-Moses and Schooling 2015). The vertical canopy of beech trees interacting with a higher rainfall inclination angle improved the efficiency of S_F generation (Van Stan et al.

2011). Lastly, S_F production is sometimes influenced by vapour pressure deficit. The lower the deficit, the higher the amount of S_F produced (Carlyle-Moses and Schooling 2015).

1.3 Morphological Characteristics Influencing Stemflow

Besides meteorological conditions, S_F production is regulated by tree morphological traits, with branch angle frequently cited as the primary factor (Herwitz 1987; Carlyle-Moses and Schooling 2015; McKee and Carlyle-Moses 2017). Diameter at breast height, D_{BH}, is also linked to S_F generation, through D_{BH} correlating with associated factors like branch numbers, projected canopy area, and bark relief index. Generally, larger the tree, the more S_F it produces, however the threshold depth of precipitation required to generate S_F also increases (Deguchi et al. 2006; André et al. 2008; Germer et al. 2010; Van Stan and Levia 2010; Carlyle-Moses and Schooling; 2015). Projected canopy area is also associated with S_F production (e.g. Navar 1993; Carlyle-Moses and Price 2006; Honda et al. 2014).

Other morphological variables associated with S_{Fv} and, to a lesser degree, $S_F\%$, include bark relief index, tree height, stem inclination, and number of branches (Honda et al. 2014, Levia et al. 2015, McKee and Carlyle-Moses 2017, Pinos et al. 2021; Su et al. 2023; Norozi et al. 2024). Bark relief index correlates negatively with S_F in multi-leader trees but positively in single-leader trees (Carlyle-Moses and Schooling 2015). This is attributed to increased storage capacity per unit area and greater surface area for the negative correlation, and the possible influence of linear furrows for the positive correlation. Stemflow decreases with greater tree height, stem inclination, and number of branches (McKee and Carlyle-Moses 2017).

1.4 Stemflow Infiltration Area

Recently, research has focused on S_F infiltration into soil. The concentrated water flow at a plant's base influences overland flow and spatial infiltration patterns. The size and shape of the stemflow infiltration area (I_t) vary based on tree species, canopy structure, soil properties, and precipitation characteristics (Van Stan and Allen 2020; Carlyle-Moses et al. 2020), owing to how these factors affect S_F generation, as well as subsurface processes. Infiltration area has been associated with several soil characteristics, including saturated hydraulic conductivity, bulk density, organic matter content, and soil texture (Schwarzel et

al. 2012, Tischer et al. 2020, Metzger et al. 2021, Llorens et al. 2022). Higher saturated hydraulic conductivity (K_{sat}) reduces I_t because water moves vertically through preferential flow paths (Schwarzel et al.2012). As bulk density rises, K_{sat} falls, suggesting that higher bulk density increases I_t. Llorens et al. (2022) also propose that elevated organic matter and larger soil texture, both associated with increased K_{sat}, result in smaller I_t. With the recent increase in studies on S_F generation and I_t, there is a distinct growing subfield on where S_F goes after it infiltrates the soil. Many studies have hypothesized that S_F is a point-source input into groundwater recharge (Tanaka et al. 1996; Taniguchi et al. 1996; Tanaka 2011; Pinos et al. 2023). However, until recently, few studies have investigated the pathways stemflow takes once infiltrated (e.g. Johnson and Lehmann 2006; Metzger et al. 2021, Hemr et al. 2023). Since the correlation in Hemr et al. (2023)'s study was highest in the topmost layer (0 cm) and lowest layer (-100 cm) measured, this suggests that S_F-initiated preferential flow may result in a point-source input of water into the soil.

Relative to other tree species, ponderosa pine (*Pinus ponderosa* Douglas ex C. Lawson) remains understudied in terms of S_F and I_t. This may, in part, be due to early studies suggesting that S_F is negligible compared to throughfall (Johnson 1942). However, three studies on Ponderosa pine found S_F represents 3-4% of season-long rainfall (Rowe and Hendrix 1951, Orr 1972, Licata et al. 2011). Ponderosa pine is a taproot species, meaning its roots penetrate deep into the soil (Province of British Columbia, 2023). This is a survival mechanism that makes ponderosa very drought-tolerant (Oliver et al. 1990), and, in conjunction with the assumption that S_F is a point-source input of water, also has implications for how S_F contributes to tree survival during droughts and in semi-arid areas. While no studies were identified that have evaluated the funneling ratios or the size of S_F's I_t around *Pinus ponderosa*, other types of forests with stemflow representing 3-4% of season-long rainfall tend to far exceed unity in funneling ratios. Therefore, the depth of S_F's infiltration may be much larger than that of bulk rainfall depth and may have implications for tree survivability (Carlyle-Moses et al. 2018).

The primary objective of this study was to determine the importance of S_F to isolated *Pinus ponderosa*. More specifically, I aimed:

i) determine the stemflow volumes, the percentage of rainfall partitioned into S_F, and the associated funneling ratio values at the rainfall event and season long times scales; ii) evaluate the tree characteristics and meteorological factors influencing this S_F production; iii) derive the rainfall threshold depths required for S_F generation and the S_F flow rates once this threshold rain depth has been reached, and iv) use the S_F flow rates obtained by meeting objective iii to simulate S_F delivery to the soil surface next to the boles of ponderosa pine to estimate the S_F infiltration areas and the equivalent depth of S_F infiltration.

1.5 References

Aboal, J. R., D. Morales, M. Hernández, and M. S. Jimènez (1999), The Measurement and Modelling of the Variation of Stemflow in A Laurel Forest in Tenerife, Canary Islands, *Journal of Hydrology,* 221(3–4), 161–175. https://doi.org/10.1016/S0022-1694(99)00086-4

Andersson, T. (1991). Influence of stemflow and throughfall from common oak (Quercusrobur) on soil chemistry and vegetation patterns. *Canadian Journal of Forest Research*, *21*(6), 917–924. https://doi.org/10.1139/x91-127

André, F., Jonard, M., & Ponette, Q. (2008). Influence of species and rain event characteristics on stemflow volume in a temperate mixed oak–beech stand. *Hydrological Processes*, *22*(22), 4455–4466. https://doi.org/10.1002/hyp.7048

Brown Jr., J. H., & Barker Jr., A. C. (1970). An analysis of throughfall and stemflow in mixed oak stands. *Water Resources Research*, *6*(1), 316–323. https://doi.org/10.1029/WR006i001p00316

Carlyle-Moses, D. E. (2004). Throughfall, stemflow, and canopy interception loss fluxes in a semi-arid Sierra Madre Oriental matorral community. *Journal of Arid Environments*, *58*(2), 181–202. https://doi.org/10.1016/S0140-1963(03)00125-3

Carlyle-Moses, D. E., Iida, S., Germer, S., Llorens, P., Michalzik, B., Nanko, K., Tischer, A., & Levia, D. F. (2018). Expressing stemflow commensurate with its ecohydrological importance. *Advances in Water Resources*, *121*, 472–479. https://doi.org/10.1016/j.advwatres.2018.08.015

Carlyle-Moses, D. E., Iida, S., Germer, S., Llorens, P., Michalzik, B., Nanko, K., Tanaka, T., Tischer, A., & Levia, D. F. (2020). Commentary: What we know about stemflow's infiltration area. *Frontiers in Forests and Global Change*, *3*. https://www.frontiersin.org/article/10.3389/ffgc.2020.577247

Carlyle-Moses, D. E., & Price, A. G. (2006). Growing-season stemflow production within a deciduous forest of southern Ontario. *Hydrological Processes*, 20(17), 3651–3663. https://doi.org/10.1002/hyp.6380

Carlyle-Moses, D. E., & Price, A. G. (2007). Modelling canopy interception loss from a Madrean pine-oak stand, northeastern Mexico. *Hydrological Processes*, *21*(19), 2572–2580. https://doi.org/10.1002/hyp.6790

Carlyle-Moses, D. E., & Schooling, J. T. (2015). Tree traits and meteorological factors influencing the initiation and rate of stemflow from isolated deciduous trees. *Hydrological Processes*, *29*(18), 4083–4099. https://doi.org/10.1002/hyp.10519

Chang, S.-C., & Matzner, E. (2000). The effect of beech stemflow on spatial patterns of soil solution chemistry and seepage fluxes in a mixed beech/oak stand. *Hydrological Processes*,

14(1), 135–144. https://doi.org/10.1002/(SICI)1099-1085(200001)14:1<135::AID-HYP915>3.0.CO;2-R

de Lima, J. A., Van Stan II, J. T., Lewińska, K., Dradrach, A., Ceglarek, J., & Tonello, K. C. (2026). Stemflow Dynamics in the Jamari National Forest (Brazilian Amazon): II. Solute Concentrations and Flux Dynamics. *Biotropica*, *58*(2), e70193. https://doi.org/10.1111/btp.70193

Deguchi, A., Hattori, S., & Park, H.-T. (2006). The influence of seasonal changes in canopy structure on interception loss: application of the revised Gash model. *Journal of Hydrology*, *318*(1), 80–102. https://doi.org/10.1016/j.jhydrol.2005.06.005

Durocher, M. G. (1990). Monitoring spatial variability of forest interception. *Hydrological Processes*, *4*(3), 215–229. https://doi.org/10.1002/hyp.3360040303

Germer, S. (2013). Development of near-surface perched water tables during natural and artificial stemflow generation by babassu palms. *Journal of Hydrology*, *507*, 262–272. https://doi.org/10.1016/j.jhydrol.2013.10.026

Germer, S., Neill, C., Krusche, A. v., & Elsenbeer, H. (2010). Influence of land-use change on near-surface hydrological processes: undisturbed forest to pasture. *Journal of Hydrology*, *380*(3–4), 473–480. https://doi.org/10.1016/J.JHYDROL.2009.11.022

Guo, M., He, J., Dong, K., Yang, N., Li, Y., Xiao, J., & Feng, L. (2022). Factors influencing maize (Zea mays) stemflow in Western Liaoning, China. *Agronomy Journal*. https://doi.org/10.1002/agj2.21234

Hemr, O., Vichta, T., Brychtova, M., Kupec, P., Žižlavská, N., Tomášová, G., & Deutscher, J. (2023). Stemflow infiltration hotspots near-tree stems along a soil depth gradient in a mixed oak–beech forest. *European Journal of Forest Research*, *142*, 1–16. https://doi.org/10.1007/s10342-023-01592-7

Herwitz, S. R. (1987). Raindrop impact and water flow on the vegetative surfaces of trees and the effects on stemflow and throughfall generation. *Earth Surface Processes and Landforms*, *12*(4), 425–432. https://doi.org/10.1002/esp.3290120408

Herwitz, S. R. (1991). Aboveground adventitious roots and stemflow chemistry of Ceratopetalum virchowii in an Australian Montane tropical rain forest. *Biotropica*, *23*(3), 210–218. https://doi.org/10.2307/2388197

Hofhansl, F., Wanek, W., Drage, S., Huber, W., Weissenhofer, A., & Richter, A. (2012). Controls of hydrochemical fluxes via stemflow in tropical lowland rainforests: Effects of meteorology and vegetation characteristics. *Journal of Hydrology*, *452–453*, 247–258. https://doi.org/10.1016/j.jhydrol.2012.05.057

Honda, E. A., Mendonça, A. H., & Durigan, G. (2014). Factors affecting the stemflow of trees in the Brazilian Cerrado. *Ecohydrology*, *8*(7), 1351–1362. https://doi.org/10.1002/eco.1587

Johnson, W. M. (1942). The interception of rain and snow by a forest of young ponderosa-pine. *Eos, Transactions American Geophysical Union*, *23*(2), 566–570. https://doi.org/10.1029/TR023i002p00566

Katul, G. G., Keshavarz, B., Meydani, A., & Levia, D. F. (2025). Stemflow Hydrodynamics. *Reviews of Geophysics*, *63*(3), e2024RG000857. https://doi.org/10.1029/2024RG000857

Kuraji, K., Tanaka, Y., Tanaka, N., & Karakama, I. (2001). Generation of stemflow volume and chemistry in a mature Japanese cypress forest. *Hydrological Processes*, *15*(10), 1967–1978. https://doi.org/10.1002/hyp.250

Levia, D. F., & Frost, E. E. (2003). A review and evaluation of stemflow literature in the hydrologic and biogeochemical cycles of forested and agricultural ecosystems. *Journal of Hydrology*, *274*(1), 1–29. https://doi.org/10.1016/S0022-1694(02)00399-2

Levia, D. F., & Germer, S. (2015). A review of stemflow generation dynamics and stemflow-environment interactions in forests and shrublands. In *Reviews of Geophysics* (Vol. 53, Issue 3, pp. 673–714). Blackwell Publishing Ltd. https://doi.org/10.1002/2015RG000479

Levia, D. F., Katul, G. G., Meydani, A., Nanko, K., Yuan, C., Zhang, Y., Llorens, P., & Bruen, M. (2025). Towards smarter green infrastructure: Fusing bark ecology and stemflow hydrodynamics on tree stems. *Ecological Indicators, 178,* 113827. https://doi.org/10.1016/j.ecolind.2025.113827

Levia, D. F., Michalzik, B., Näthe, K., Bischoff, S., Richter, S., & Legates, D. R. (2015). Differential stemflow yield from European beech saplings: the role of individual canopy structure metrics. *Hydrological Processes*, *29*(1), 43–51. https://doi.org/10.1002/hyp.10124

Levia, D. F., Van Stan, J. T., Mage, S. M., & Kelley-Hauske, P. W. (2010). Temporal variability of stemflow volume in a beech-yellow poplar forest in relation to tree species and size. *Journal of Hydrology*, *380*(1–2), 112–120. https://doi.org/10.1016/j.jhydrol.2009.10.028

Licata, J. A., Pypker, T. G., Weigandt, M., Unsworth, M. H., Gyenge, J. E., Fernández, M. E., Schlichter, T. M., & Bond, B. J. (2011). Decreased rainfall interception balances increased transpiration in exotic ponderosa pine plantations compared with native cypress stands in Patagonia, Argentina. *Ecohydrology*, *4*(1), 83–93. https://doi.org/10.1002/eco.125

Llorens, P., Latron, J., Carlyle-Moses, D. E., Näthe, K., Chang, J. L., Nanko, K., Iida, S., & Levia, D. F. (2022). Stemflow infiltration areas into forest soils around American beech (Fagus grandifolia Ehrh.) Trees. *Ecohydrology*, *15*(2). https://doi.org/10.1002/eco.2369

McKee, A. J., & Carlyle-Moses, D. E. (2017). Modelling stemflow production by juvenile lodgepole pine (Pinus contorta var. Latifolia) trees. *Journal of Forestry Research*, *28*(3), 565–576. https://doi.org/10.1007/s11676-016-0336-9

Metzger, J. C., Filipzik, J., Michalzik, B., & Hildebrandt, A. (2021). Stemflow infiltration hotspots create soil microsites near tree stems in an unmanaged mixed beech forest. *Frontiers in Forests and Global Change*, *4*. https://doi.org/10.3389/ffgc.2021.701293

Muoghalu, J. I. (2003). Contributions of throughfall, stemflow and litterfall to nutrient cycling in a secondary lowland rain forest in Ile-Ife, Nigeria. *Journal of Tropical Forest Science*, *15*(3), 399–410. https://www.jstor.org/stable/23616441

Návar, J. (1993). The causes of stemflow variation in three semi-arid growing species of northeastern Mexico. *Journal of Hydrology*, *145*(1), 175–190. https://doi.org/10.1016/0022-1694(93)90226-Y

Norozi, A., Attarod, P., Pypker, T. G., Sadeghi, S. M. M., & Etemad, V. (2024). Estimation of bark water storage capacity of broad- and needle-leaved trees planted in a semi-arid climate zone. *Journal of Arid Environments*, *220*, 105100. https://doi.org/10.1016/j.jaridenv.2023.105100

Oliver WW, Ryker RA (1990) Silvics of ponderosa pine. In: Burns R.M., Honkala B.H., tech. coords [eds.], *Silvics of North America, Volume 1, Conifers. Agriculture Handbook. 654,* 413–424. Forest Service, U.S. Department of Agriculture, Washington, DC, pp 413–424. https://research.fs.usda.gov/silvics/ponderosa-pine

Orr, H. K., & Rocky Mountain Forest and Range Experiment Station (Fort Collins, Colo.). (1972). *Throughfall and stemflow relationships in second-growth ponderosa pine in the black hills*. Rocky Mountain Forest and Range Experiment Station, Forest Service, U.S. Department of Agriculture. https://books.google.ca/books?id=nJ_wiNy68v4C

Parker, G. G. (1983). Throughfall and stemflow in the forest nutrient cycle. In A. MacFadyen & E. D. Ford (Eds.), *Advances in Ecological Research* (Vol. 13, pp. 57–133). Academic Press. https://doi.org/10.1016/S0065-2504(08)60108-7

Pinos, J., Latron, J., Levia, D. F., & Llorens, P. (2021). Drivers of the circumferential variation of stemflow inputs on the boles of Pinus sylvestris L. (scots pine). *Ecohydrology*, *14*(8), e2348. https://doi.org/10.1002/eco.2348

Pinos, J., Flury, M., Latron, J., & Llorens, P. (2023). Routing stemflow water through the soil via preferential flow: a dual-labelling approach with artificial tracers. *Hydrology and Earth System Sciences*, *27*(15), 2865–2881. https://doi.org/10.5194/hess-27-2865-2023

Price, A. G., & Carlyle-Moses, D. (2004). Measurement and modelling of growing-season canopy water fluxes in a mature mixed deciduous forest stand, southern Ontario, Canada.

Agricultural and Forest Meteorology, *119*, 69–85. https://doi.org/10.1016/S0168-1923(03)00117-5

Rowe, P. B., & T. M. Hendrix. (1951). Interception of rain and snow by second-growth ponderosa pine. *Eos, Transactions American Geophysical Union*, *32*(6), 903–908. https://doi.org/10.1029/TR032i006p00903

Schooling, J. T., & Carlyle-Moses, D. E. (2015). The influence of rainfall depth class and deciduous tree traits on stemflow production in an urban park. *Urban Ecosystems*, *18*(4), 1261–1284. https://doi.org/10.1007/s11252-015-0441-0

Schwärzel, K., Ebermann, S., & Schalling, N. (2012). Evidence of double-funneling effect of beech trees by visualization of flow pathways using dye tracer. *Journal of Hydrology*, *470–471*, 184–192. https://doi.org/10.1016/j.jhydrol.2012.08.048

Spencer, S. A., & van Meerveld, H. J. (2016). Double funnelling in a mature coastal British Columbia forest: spatial patterns of stemflow after infiltration. *Hydrological Processes*, *30*(22), 4185–4201. https://doi.org/10.1002/hyp.10936

Staelens, J., de Schrijver, A., & Verheyen, K. (2007). Seasonal variation in throughfall and stemflow chemistry beneath a European beech (Fagus sylvatica) tree in relation to canopy phenology. *Canadian Journal of Forest Research*, *37*(8), 1359–1372. https://doi.org/10.1139/X07-003

Staelens, J., de Schrijver, A., Verheyen, K., & Verhoest, N. E. C. (2008). Rainfall partitioning into throughfall, stemflow, and interception within a single beech (Fagus sylvatica L.) canopy: influence of foliation, rain event characteristics, and meteorology. *Hydrological Processes*, *22*(1), 33–45. https://doi.org/10.1002/hyp.6610

Su, L., Qi, L., Zhuang, W., & Zhang, Y. (2023). Contrasting effects of low-severity fire on stemflow production between coexisting pine and oak trees. *Science of The Total Environment*, *858*, 159885. https://doi.org/10.1016/j.scitotenv.2022.159885

Tanaka, T. (2011). Effects of the canopy hydrologic flux on groundwater. In: Levia, D., Carlyle-Moses, D., Tanaka, T. [eds.], *Forest Hydrology and Biogeochemistry. Ecological Studies, vol 216.* Springer, Dordrecht. https://doi.org/10.1007/978-94-007-1363-5_25

Tanaka, T., Taniguchi, M., & Tsujimura, M. (1996). Significance of stemflow in groundwater recharge. 2: A cylindrical infiltration model for evaluating the stemflow contribution to groundwater recharge. *Hydrological Processes*, *10*(1), 81–88. https://doi.org/10.1002/(SICI)1099-1085(199601)10:1<81::AID-HYP302>3.0.CO;2-M

Taniguchi, M., Tsujimura, M., & Tanaka, T. (1996). Significance of stemflow in groundwater recharge. 1: Evaluation of the stemflow contribution to recharge using a mass balance approach. *Hydrological Processes*, *10*(1), 71–80. https://doi.org/10.1002/(SICI)1099-1085(199601)10:1<71::AID-HYP301>3.0.CO;2-Q

Tischer, A., Michalzik, B., & Lotze, R. (2020). Nonuniform but highly preferential stemflow routing along bark surfaces and actual smaller infiltration areas than previously assumed: A case study on European beech (Fagus sylvatica L.) and sycamore maple (Acer pseudoplatanus L.). *Ecohydrology*, *13*(6). https://doi.org/10.1002/eco.2230

Van Stan, J. T., & Allen, S. T. (2020). What we know about stemflow's infiltration area. *Frontiers in Forests and Global Change*, *3*. https://doi.org/10.3389/ffgc.2020.00061

Van Stan, J. T., & Levia, D. F. (2010). Inter- and intraspecific variation of stemflow production from Fagus grandifolia Ehrh. (American beech) and Liriodendron tulipifera L. (yellow poplar) in relation to bark microrelief in the eastern united states. *Ecohydrology*, *3*(1), 11–19. https://doi.org/10.1002/eco.83

Van Stan, J. T., Siegert, C. M., Levia, D. F., & Scheick, C. E. (2011). Effects of wind-driven rainfall on stemflow generation between codominant tree species with differing crown characteristics. *Agricultural and Forest Meteorology*, *151*(9), 1277–1286. https://doi.org/10.1016/j.agrformet.2011.05.008

Van Stan, J. T., Van Stan, J. H., & Levia, D. F. (2014). Meteorological influences on stemflow generation across diameter size classes of two morphologically distinct deciduous species. *International Journal of Biometeorology*, *58*(10), 2059–2069. https://doi.org/10.1007/s00484-014-0807-7

Wagner, S., Brantley, S., Stuber, S., Van Stan, J., Whitetree, A., & Stubbins, A. (2019). Dissolved black carbon in throughfall and stemflow in a fire-managed longleaf pine woodland. *Biogeochemistry*, *146*(2), 191–207. https://doi.org/10.1007/s10533-019-00620-2

Wu, M.-D., Jiang, Z.-Y., Yang, X., Yeerbolati, B., Huang, L., Zhong, Y.-Y., Zhang, H.-W., & Li, X.-Y. (2024). Global quantitative synthesis on the patterns and drivers of funneling ratio and enrichment ratio for stemflow. CATENA, 244, 108253. https://doi.org/10.1016/j.catena.2024.108253

Xiao, Q., E. G. McPherson, S. L. Ustin, M. E. Grismer, and J. R. Simpson (2000), winter rainfall interception by two mature open-grown trees in Davis, California. *Hydrological Processes*, 14(4), 763–784, https://doi.org/10.1002/(SICI)1099-1085(200003)14:4<763::AID-HYP971>3.0.CO;2-7

Zabret, K., Rakovec, J., & Šraj, M. (2018). Influence of meteorological variables on rainfall partitioning for deciduous and coniferous tree species in urban area. *Journal of Hydrology*, *558*, 29–41. https://doi.org/10.1016/j.jhydrol.2018.01.025

Zuecco, G., Marchina, C., Censini, M., Todini-Zicavo, D., Cassiani, G., & Borga, M. (2025). A simple experiment to trace stemflow infiltration: advantages and challenges of using stable isotopes of hydrogen and oxygen and electrical resistivity tomography. *Vadose Zone Journal*, *24*(1), e20397. https://doi.org/10.1002/vzj2.20397

Chapter 2: Stemflow Production from Isolated Ponderosa Pine (*Pinus ponderosa*) and its Subsequent Infiltration in a Semi-Arid Landscape

2.1 Introduction

Tree canopies can considerably alter the spatial delivery of rainfall reaching the ground by partitioning rainfall into throughfall - rainfall that passes through canopy gaps or drips from the canopy - and stemflow, S_F - rainfall that directly strikes a tree bole or is routed to that bole from the canopy where it subsequently flows to the ground. Although S_F may be quantitatively insignificant at the forest stand and watershed scales, often representing <5% of rainfall (see Silva & Rodríguez, 2001; Fan et al., 2015; Zhang et al., 2020), the concentrated nature of this input at the base of trees may mean that the hydrological and biogeochemical role of S_F is not inconsequential (Levia & Frost, 2003; Levia & Germer, 2015; Carlyle-Moses et al., 2018). For example, once S_F has infiltrated into the soil it can travel as preferential by-pass flow following tree roots and macropores (Martinez-Meza & Whitford, 1996; Johnson & Lehmann, 2006; Pinos et al., 2023). Consequently, S_F may be an important source of groundwater (Taniguchi et al., 1996; Tanaka et al. 1996) and deep-soil moisture rechange (Pressland, 1976; Buttle et al., 2014; Spencer & van Meerveld, 2016; Hemr et al., 2023). Additionally, S_F has been shown to enhanced nutrient input into near-stem soils (Chang & Matzner, 2000; Staelens et al., 2007; Mantovani et al., 2022), the generation of perched water tables (Germer, 2013), as well as the development of distinct soil microsites where certain physical properties of near-stem soils (e.g., clay content, soil structure consolidation, and macropore fraction) differ from those of soils distal to the bole (Metzger et al., 2021). As such, S_F as a “hot spot” and “hot moment” of water and solute inputs represents a link between vegetation canopies and the critical zone (McClain et al., 2003). Despite accounting for a small fraction of the total precipitation input to watersheds, there is an ever-increasing body of research suggesting the role of S_F in the hydrological and biogeochemical cycles of forested areas is far from negligible (see Parker, 1983; Levia & Frost, 2003; Levia & Germer, 2015; Carlyle-Moses et al., 2018; Metzger et al. 2021).

Historically, the quantitative importance of S_F has been expressed by reporting the percentage of bulk rainfall partitioned into this water flux at the forest plot scale (Brown & Barker, 1970; Lloyd & Marques, 1988; Johnson, 1990) or, in the case of individual trees, the percentage of rainfall that would have fallen on the tree's crown area (e.g., Guevara-Escobar et al. 2007; Honda & Durigan, 2016). However, quantifying S_F as a fraction of bulk precipitation either at the forest stand or individual tree crown scales masks the volumetric importance of S_F input at the scale in which it reaches the soil surface and enters the subsoil. The S_F funnelling ratio (F, dimensionless) (Herwitz, 1986), which relates the volume of rainfall partitioned into S_F by a tree to the volume of rainfall that would have been captured by a rain gauge having an orifice area equal to that of the tree's basal area, has been commonly used to quantify the concentration effect trees have in routing S_F to their bases (e.g., Carlyle-Moses & Price, 2007; González-Martinez et al., 2017; Zhang et al., 2020). For example, Van Stan & Levia (2010) found that mean study-period F values for American beech (*Fagus grandifolia*) and yellow poplar (*Liriodendron tulipifera*) were 37.4 and 12.2 across all tree sizes in a forested stand in Maryland, USA, while McKee & Carlyle-Moses (2017) derived mean study-period F values for two plots of juvenile lodgepole pine (*Pinus contorta*) of 22.2 and 23.4 with a single-event, single-tree maximum F of 111.7 (rain depth = 17.3 mm, tree bole diameter = 3.3 cm). Although a better representation of the quantitative importance of S_F at the sub-stand scale, F values still do not provide forest hydrologists, biogeochemists and others interested in vegetation-atmosphere-soil interactions with the requisite information to simulate S_F's role in critical zone hydrology and biogeochemistry. That is, the F_R metric does not provide the depth of infiltrated S_F nor the area over which that infiltration occurs. However, Levia and Germer (2015) and Carlyle-Moses et al. (2018) made suggestions for how to do so by substituting the tree basal area with the tree-scale infiltration area.

The area of near-stem soil in which S_F infiltrates - i.e., the stemflow infiltration area (I_t, m^2) is beginning to garner increased research attention (e.g., Tischer et al., 2020; Metzger et al., 2021; Llorens et al. 2022). Although $I_T > 1$ m^2 for a single tree may occur under extreme rainfall conditions in certain environments (see Pressland, 1973; Herwitz, 1986), the results from studies using direct observations (e.g., Durocher, 1990; Návar, 2011), dye experiments (Schwärzel et al., 2012; Tischer et al., 2020), and dividing the S_F rate by the saturated hydraulic conductivity (K_{sat}, mm h^{-1}) of the soil surface (e.g., Gomez et al., 2002; Carlyle-Moses et al.,

2018) all suggest that I_t is often much less than 1 m^2 . This is not surprising since forest soils tend to have relatively high K_{sat} (i.e., > 100 mm h^{-1} and sometimes > 1000 mm h^{-1}), while mean S_F input rates to forest soils tend to be within the 1 x 10^{-2} to 1 x 10^{0} L h^{-1} range (Carlyle-Moses et al., 2018). Stemflow volumes, and thus by extension S_F flow rates, have been shown to be dependent on both tree characteristics and during rainfall event meteorological variables which may have differing impacts on S_F production depending on the tree species and or size of tree (Van Stan et al., 2014; Schooling & Carlyle-Moses, 2015). Tree characteristics that have been shown to influence the amount of S_F generated include if the tree has a single, principle leader or if it has multiple leaders extending from the crown base; tree diameter at breast height; tree height; bark texture; branching angle; crown diameter; crown height to width ratio; degree of foliation; proximity to neighbouring trees and tree lean (e.g., Levia et al., 2015; McKee & Carlyle-Moses, 2017; Cayuela et al., 2018; Pinos et al., 2021; Tonello et al., 2021; Su et al., 2023). During rainfall meteorological factors that have been found to exert a control on F include rainfall depth, intensity, and duration; the duration and frequency of rainfall breaks during the rain event; wind velocity; rainfall inclination angle, and vapour pressure deficit (e.g., Staelens et al., 2008; Van Stan et al., 2014; Carlyle-Moses & Schooling, 2015; Zabret et al., 2018). As such, the rate of S_F delivery to the critical zone and the area over which S_F infiltration occurs is dependent on tree characteristics and the meteorological conditions during the rain event. Thus, determining the associations between S_F production and tree + meteorological factors is an important consideration when assessing the linkages between the atmosphere, tree canopy, and the critical zone as well as understanding how these linkages may differ due to changes in vegetation cover or climate.

Ponderosa pine (*Pinus ponderosa* Douglas ex C. Lawson), also known as yellow pine, western yellow pine, bull pine, and rock pine (Oliver & Ryker, 1990; Parish et al., 1996), is a large conifer (to 15 – 30 m tall) native to western North America where five subspecies are recognized (Callaham, 2013). The boles of ponderosa pine are typically straight with a slight taper, while the crown may be described as symmetrical, broad, and open. The evergreen needles of these trees occur in bundles of three, are flexible, thin, and are 10-20 cm in length (Parish et al, 1996). The bark of ponderosa pine is scaley when young, becoming deeply incised with fissures separated by puzzle-shaped plates that are easily flaked on mature trees (Parish et al., 1996). Ponderosa pine is one of the most drought resistant trees in North America (Oliver

et al., 1990) and is commonly exposed to wildfire. Although seedlings are often killed by fire, the thick bark and self-pruning of the lower branches by mature trees protects against ground fires and the spread of fire to the upper canopy (Parish et al, 1996; Fryer, 2018). The subspecies *P. ponderosa* var. *ponderosa* (Douglas ex C. Lawson), also known as Columbia ponderosa pine (Callaham, 2013), extends into Canada where it is confined to the south-central interior of the province of British Columbia (Government of Canada, 2015). Within the southern interior of British Columbia ponderosa pine as a climax species occurs from low elevation, semi-arid valley bottoms to an elevation of approximately 900 m above sea level although it can extend to approximately 1500 m above sea level on dry southern exposures (Parish et al., 1996). Due to frequent ground and crown fires ponderosa pine grows predominantly in pure stands comprised of several small, even-aged cohorts (Province of British Columbia, 2023). At the lower elevation extent of its range in British Columbia ponderosa pine form open-canopy, savanna-like communities (Meidinger & Pojar, 1991) where grasses and shrubs typically dominate areas comprised of fine textured soils (Province of British Columbia, 2023). Areas with coarse-textured soils favour ponderosa pine establishment and growth since these soils permit higher permeability, deeper water penetration, and greater water storage at depth where it may be reached only by the roots of these trees. Ponderosa pine develop tap roots, with these roots extending to depths >2 m for mature trees, especially in coarse-textured soils. In open canopy stands lateral roots of mature trees may spread > 40 m with the main root mass being concentrated within 0.6 m of the surface (Province of British Columbia, 2023).

Although ponderosa pine represents the most widely distributed pine species in western North America, extending from Canada to northern Mexico (Petrides, 1998), information concerning S_F from this species is limited. This dearth of S_F information may, in part, be due to early studies conducted in ponderosa pine and other coniferous stands suggesting S_F is an insignificant component of the water balance of these forests since it represents a small fraction of stand-scale rainfall (e.g., Johnson, 1942; see McKee, 2010). However, studies that have evaluated ponderosa pine S_F in thinned and un-thinned second-growth stands (Rowe & Hedrix, 1951; Orr, 1972) or in exotic plantations (Licata et al., 2011) have found that S_F represents approximately 3 to 4% of bulk season-long rainfall, a value that falls within mid- to mid-high-range of S_F percentages when all forest types globally are considered (McKee, 2010; Van Stan and Gordon, 2018; Zhang et al., 2021) and in agreement with the mean value of 4.2% from the

review of 50 stemflow studies conducted in *Pinus* genera forests by McKee (2010). Although no studies to my knowledge have derived F values for ponderosa pine or evaluated the size of I_t around the boles of these trees, forests with S_F constituting 3 to 4% of season-long or annual rainfall are likely to have funneling ratios that far exceed unity (Carlyle-Moses et al., 2018) and as such the depths of S_F input around the boles of ponderosa pine may be much greater than bulk rainfall depths, depending on the infiltrability of the near-stem soil.

The objectives of this study, in a semi-arid ponderosa pine park-like ecosystem of south-central British Columbia, were to: i) determine the S_F volumes, the percentage of rainfall partitioned into S_F, and the associated F values at the rainfall event and season long times scales; ii) evaluate the tree characteristics and meteorological factors influencing this S_F production; iii) derive the rainfall threshold depths required for S_F generation and the S_F flow rates once this threshold rain depth has been reached, and iv) use the S_F flow rates obtained by meeting objective iii to simulate S_F delivery to the soil surface proximal to the boles of ponderosa pine to estimate the S_F infiltration areas and the equivalent depth of S_F infiltration.

2.2 Materials and Methods

2.2.1 Study Area

Measurements of S_F, rainfall and during-rainfall meteorological variables were conducted on a portion of the undeveloped lands of the Thompson Rivers University campus, located in Kamloops, British Columbia, Canada (50°40′26″N, 120°22′24″W) at an elevation averaging 567 m above mean sea level (Figure 2.1). According to the high-resolution climate mapping software CLIMATEBC ver 4.72 (Wang et al., 2006; 2012), the study area has a long-term (1991–2020) mean annual precipitation depth of 297 mm (rain = 245 mm rain, snow = 52 mm) with precipitation solely falling as rain from April through mid-November, while snow and rain events occur throughout the remainder of the year (Figure 2.2). The mean annual temperature is 8.0 °C with mean monthly temperatures ranging from −3.7 °C in January to 20.0 °C in July. The Köppen climate classification for the region is BSk (cool semi-arid) while the provincial Biogeoclimatic Ecosystem Classification (BEC) designation (BC Ministry of

Forests and Range, 2008) for this site is Bunchgrass (BG) zone -very dry hot sub-zone (BGxh) (Nicholson et al., 1991).

The research plot may be described as a ponderosa pine parkland habitat dominated by big sagebrush (*Artemisia tridentata* Nutt.). Other ground vegetation includes bluebunch wheatgrass (*Pseudoroegneria spicata* (Pursh) Á. Love), Saskatoon service berry (*Amelanchier alnifolia* (Nutt.) Nutt.), Oregon grape (*Mahonia aquifolium* Pursh), and fragile prickly pear cactus (*Opuntia fragilis* (Nutt.) Haw.). The 7.0 ha study site contains 86 ponderosa pine trees ≥ 1.0 cm in diameter (stem density = 12.3 stems ha^{-1}) ranging from 1.1 – 57.8 cm with a mean diameter at breast height (D_{BH}, cm) of 15.2 cm. However, the distribution of ponderosa pine tree D_{BH} is skewed to the right (Figure 2.3) with a median value of 14.6 cm. The ponderosa pine basal area of the site is 0.30 m^2 ha^{-1}. The topography is undulating with steep rocky outcrops dominating the eastern sections, while soils are moderate to coarse textured loamy sand / sandy loam and often rocky.

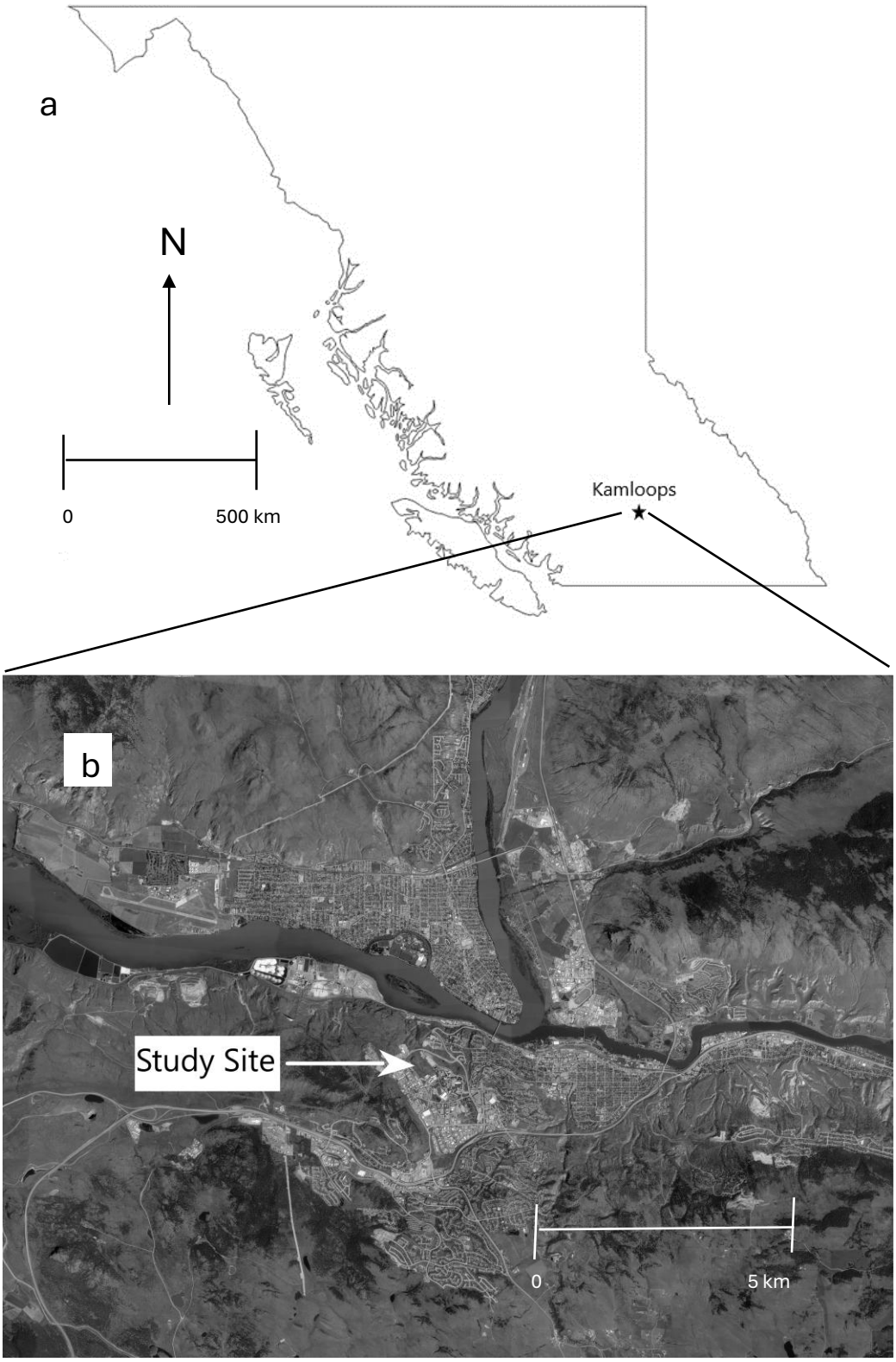

Figure 2.1: a) Geographic location of Kamloops within the Province of British Columbia, and b) location of the study plot within Kamloops (50°40′26″N, 120°22′24″W).

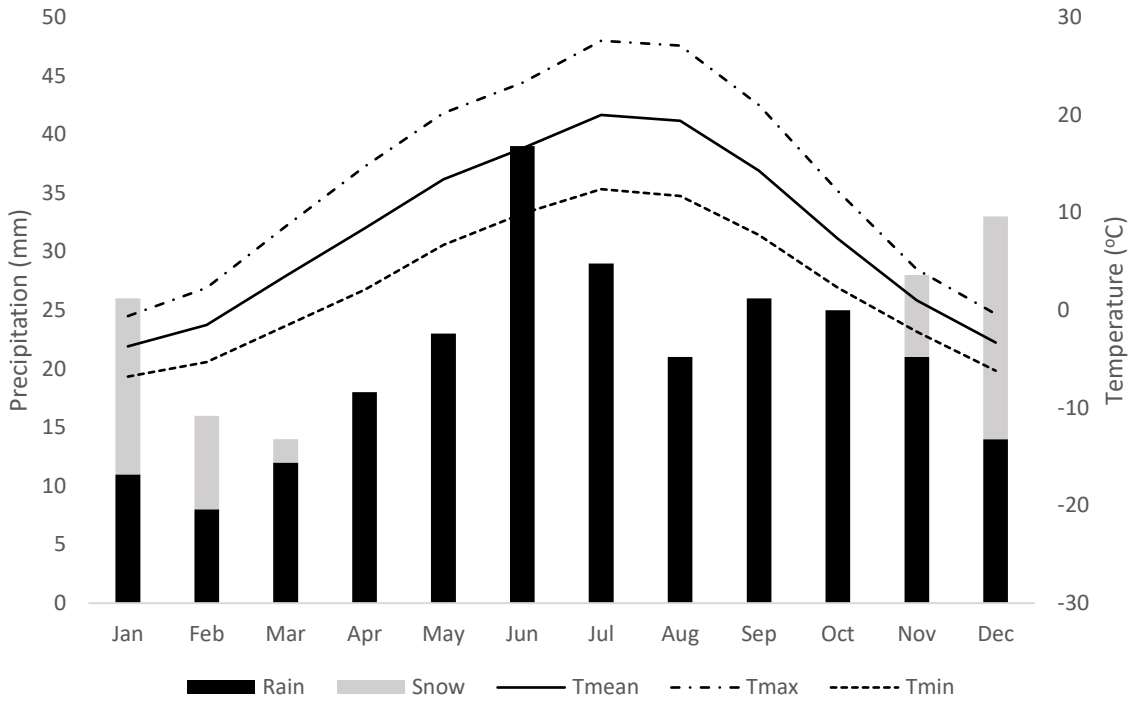

Figure 2.2: Climograph (1991 – 2020) for the ponderosa pine parkland study site. Data source: CLIMATEBC ver 4.72 (Wang et al., 2006; 2012).

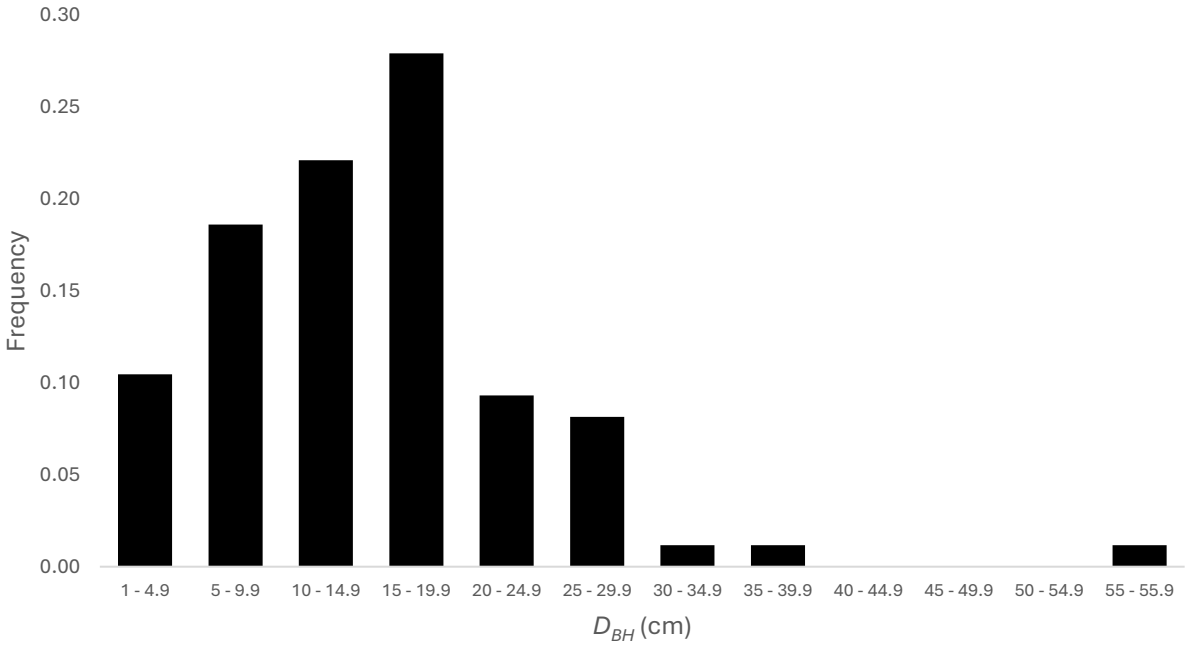

Figure 2.3: Ponderosa pine tree diameter at breast height (D_{BH}, cm) frequency distribution at the study site in Kamloops, British Columbia.

2.2.2 Tree Selection and Tree Traits

Twelve ponderosa pine trees were selected for event S_F measurement. The trees chosen were isolated – that is no other canopies from neighbouring trees extended into a field a view of a 45° cone centred at the base of the tree and had a single leader (i.e., they were not forked). The 12 trees were also selected to give a good cross-section of the tree D_{BH} distribution of the study plot. For each tree, field measurements were taken of the D_{BH} (cm); tree height (H, m), canopy height (C_H, m) and mean canopy width (C_W, m), with C_W derived from the average canopy width of each cardinal and ordinal directional span of the canopy (N-S, NE-SW, E-W and SE-NW). Based on these measured tree metrics the projected canopy area (P_{CA}, m^2) and the canopy height to width ratio ($R_{H\text{-}W}$, dimensionless) were calculated. A bark relief index (B_{RI}, dimensionless) was derived by taking the ratio of each tree's surface (furrowed) to unfurrowed circumference at breast height, with the furrowed circumference found by carefully encircling the tree's bole with a ribbon following all furrows and cracks and then subsequently measuring the length of that ribbon (see Yarranton, 1967; Van Stan et al, 2010; Carlyle-Moses & Schooling, 2015). Additionally, photographs centred at mid-canopy were taken in each of the four cardinal directions. These photographs were then analysed using ImageJ image processing software (National Institutes of Health and the Laboratory for Optical and Computational Instrumentation, LOCI, University of Wisconsin) to determine the branch count (B_N) and the average branching angle (A_B, degrees from horizontal) for each tree. These photographs were also used to determine the canopy volume of each tree (C_V, m^3) using the methods of Schooling (2014) in which side-on canopy areas (m^2) are calculated using ImageJ and divided by the canopy widths in each cardinal direction span (N-S, E-W), yielding average canopy height. Canopy volume was then found by multiplying average canopy height (m) by P_{CA}, (m^2). Table 2.1 provides the measured and derived tree traits for each of the trees in which S_F was measured.

Strong and significant ($p < 0.001$) positive correlations between D_{BH} and five other measured and derived tree traits were found (H, C_H, P_{CA}, C_V, B_N), while a weak, yet still significant ($p < 0.10$) positive relationship was found between D_{BH} and $R_{H\text{-}W}$. Mean branching angle A_B, was the only tree trait not significantly correlated with D_{BH} (Table 2.2).

Table 2.1: Traits of the 12 trees in which stemflow was measured. Terms are defined in section 2.2.4.

Tree ID	D_{BH} (cm)	H (m)	C_H (m)	$R_{H\text{-}W}$	P_{CA} (m^2)	C_V (m^3)	B_N	A_B (°)	B_{RI}
M-1	4.9	2.7	2.5	1.64	1.9	3.2	23	45	1.06
M-2	6.4	2.8	2.8	1.36	3.4	6.4	30	4	1.04
M-3	8.1	3.4	3.4	1.72	3.1	7.4	24	36	1.09
M-4	9.5	3.3	3.3	1.32	5.0	10.2	37	1	1.12
M-5	12.1	4.4	3.6	1.48	4.7	10.9	30	47	1.08
M-6	13.2	4.5	4.5	1.69	5.6	18.0	41	37	1.11
M-7	15.7	3.9	2.6	0.87	7.2	15.2	34	42	1.11
M-8	18.1	6.2	6.2	1.42	15.0	61.1	57	43	1.16
M-9	19.4	6.1	6.1	1.59	11.8	52.2	73	18	n.a. *
M-10	22.4	6.3	6.3	1.54	13.4	61.5	72	32	1.17
M-11	25.8	10.2	10.2	1.87	23.5	175.2	77	36	1.14
M-12	28.4	9.7	9.6	2.05	17.4	121.7	80	24	1.15

*Tree M-9 was removed as part of a construction project on the Thompson Rivers University Kamloops campus before B_{RI} measurements could be taken.

Table 2.2: Relationship type, correlation (R^2) and significance of the relationships between DBH and all other tree traits measured or derived for this study.

D_{BH} versus	Relationship Type	R^2	Significance
Tree Height H	Logarithmic	0.943	$p < 0.001$
Canopy Volume C_V	Logarithmic	0.941	$p < 0.001$
Projected Crown Area P_{CA}	Logarithmic	0.912	$p < 0.001$
Branch Count B_N	Linear	0.881	$p < 0.001$
Canopy Height C_H	Logarithmic	0.833	$p < 0.001$
Bark Relief Index B_{RI}	Linear	0.687	$p < 0.001$
Canopy Height to Width Ratio $R_{H\text{-}W}$	Linear	0.163	$p < 0.1$
Mean Branch Angle A_B	Logarithmic	0.084	n.s.

2.2.3 Precipitation and Stemflow Measurement

Rainfall depth was measured with an OTT Pluvio^2 L all-weather weighing precipitation gauge (Model # 05108-45) with a resolution of 0.1 mm tip^{-1} on a 5-min temporal resolution. The weighing precipitation gauge was equipped with an Alter shield and forms part of the TRU-Wx meteorological and air quality monitoring station, situated at the approximate geographic centre of the research plot (Figure 2.4). No obstructions, including the 10 m meteorological tower at the site, extended into a 45° cone of view situated at the centre of the 200 cm^2 (16.0 cm diameter) gauge opening. In addition to the weighing precipitation gauge, a

standard manually read rainfall gauge (Productive Alternatives - Stratus Rain Gauge), was situated at the TRU-Wx site, approximately 9 m from the weighing precipitation gauge with the 87.1 cm^2 (10.2 cm diameter gauge opening) placed 1 m off the ground. Four additional manually read gauges were placed around the study site to assess the spatial variability of event rainfall depth. Like the weighing precipitation gauge, no obstructions extended into a 45^o cone of view situated at the centre of each of the manually read rain gauges. Figure 2.4 shows the location of the weighing precipitation gauge, the 5 manually read gauges, and the TRU-Wx station in relation to the 12 trees used to measure S_F.

Stemflow was captured by fabricating collection collars from 2.5 cm wide corrugated polyethylene hose cut into a U-shape and wrapped twice around each of the study tree boles. One edge of the collar was affixed to the tree bole using staples and 100% silicone. The collars were angled (approximately 10^o) to promote drainage of S_F with the terminus of each hose left uncut and leading to a 20 L polyethylene pail reservoir for subsequent S_F volume measurement using a graduated cylinder. Stemflow generated by rain events that ended during daylight hours was normally measured within 2 hours of the event cessation, however, if a rain event extended into the night, S_F was measured the following morning. To minimize any evaporation of collected S_F the reservoirs were painted white and were sealed with a lid. Additionally, 5 ml of mineral oil was placed in the reservoirs between rain events so that the oil would form a barrier between the next event's collected S_F and the overlying air in the reservoir. A tree was considered to have generated S_F when S_F volume was ≥0.01 L and S_F volume was measured using a graduated cylinder.

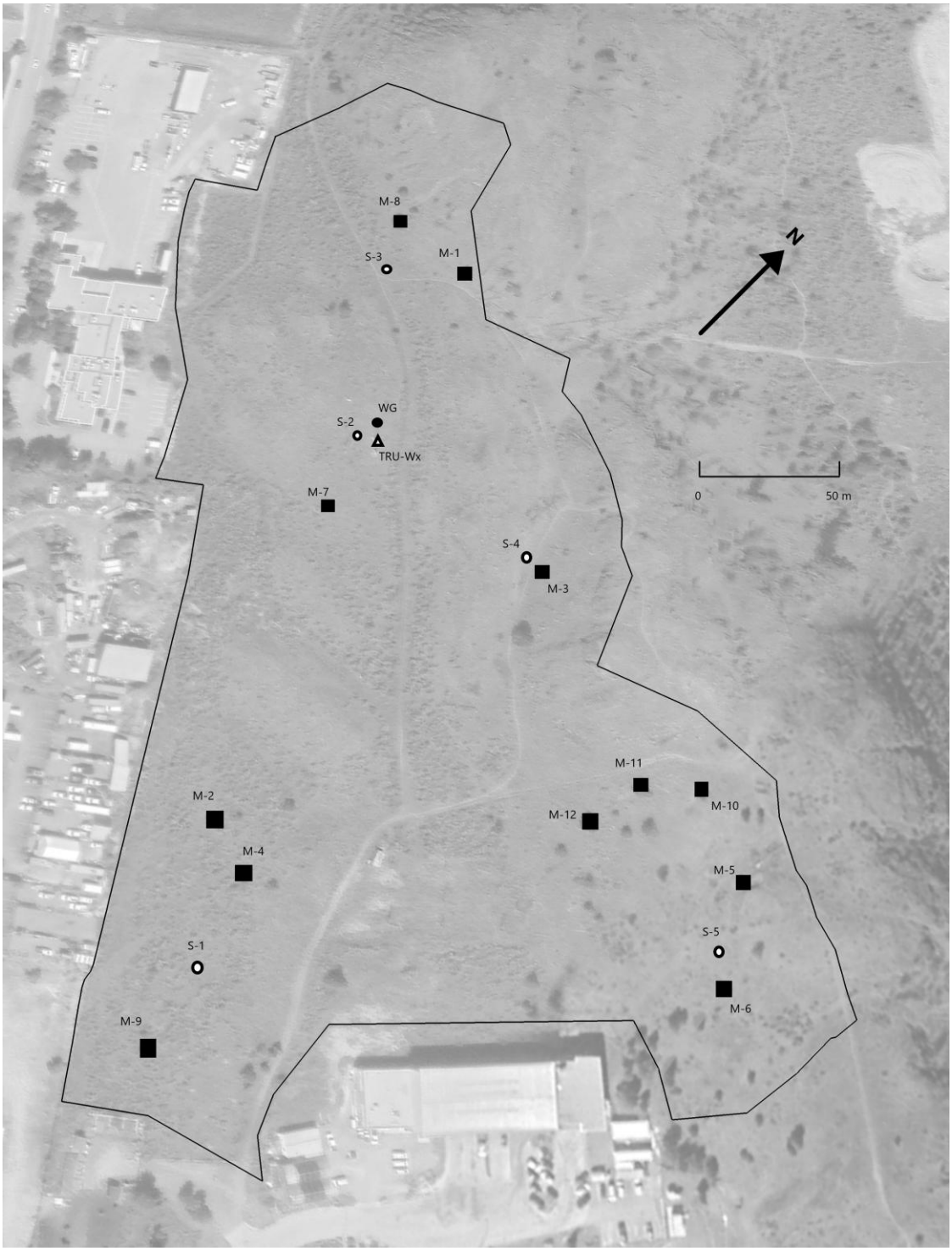

Figure 2.4: Distribution of the stemflow study trees (black squares, M-1 to M-12), standard manually read gauges (black circles with white fill, S-1 to S-5), the weighing precipitation gauge (black circle, WS) and the meteorological station (black triangle with white fill, TRU-Wx) at the study site. Thick black line = perimeter of the 7-ha study area.

2.2.4 Measurement and derivation of meteorological variables

Temperature and relative humidity were measured at 2.0 m from the ground surface at the TRU-Wx meteorological station using a Rotronic HygroClip standard climate probe (Model # HC2A-S), while wind speed and direction were measured at the meteorologic station using an RM Young Heavy-Duty Wind Monitor (Model # 05108-45) at a height of 2.2 m above the ground. Rainfall depth, temperature, relative humidity, wind speed and wind direction data were averaged over a 5-min period and transmitted from a Sutron Xlite data logger (Model # 9210-B) to the web-based HydroMet Cloud data housing site (OTT HydroMet) for subsequent retrieval.

It is now recognized that the evaporation of intercepted rainfall from vegetation canopies is due to mass transfer; that is evaporation from the canopy occurs as free water evaporation and is a function of the vapour pressure deficit between the canopy and the overlying air (*VPD*, kPa) and the aerodynamic conductance of that canopy (Stewart, 1977; Teklehaimanot et al., 1991; Pereira et al., 2009). Assuming that tree canopies, especially those of ponderosa pine in a park-like landscape, are well coupled with the atmosphere (see Pereira et al., 2009; Carlyle-Moses and Gash, 2011), the temperature of the canopy and the overlying air were assumed to be equal allowing for VPD (kPa) to be derived as:

$$VPD = [1 - H_R] \cdot 0.611 \cdot exp[(17.3 \cdot T_a) \cdot (237.3 + T_a)^{-1}] \quad \text{Eq. 2.1}$$

where H_R is the relative humidity of the air expressed as a ratio, and T_a is the air temperature (°C).

Since the roughness of a canopy may be considered stable over the course of a single growing season, variations in aerodynamic conductance are entirely due to differences in wind speed. As such, an evaporation coefficient (E, kPa m s^{-1}) that quantifies the during rain event evaporation rate from the canopy can be derived as the product of VPD (kPa) and wind speed (v_a, m s^{-1}) (see Carlyle-Moses and Schooling, 2015):

$$E = VPD \cdot v_a \quad \text{Eq. 2.2}$$

The weighing precipitation gauge record was used to identify the start and end of each rain event, with a rain event being defined as a period of rainfall bounded by at least 12 h of no rainfall ≥0.2 mm. The 12 h period was selected as it was assumed to be enough time to allow the canopies to completely dry (eliminating the influence of partially wetted canopies in my analysis), and to allow time to conduct S_F measurements. The duration of intra-storm breaks (≥ 0.5 h with no measurable rainfall) was also derived from the weighing precipitation gauge record yielding the total duration of intra-storm breaks for an event (D_B, h) and the total rain duration (D_R, h). Two measures of rainfall intensity were derived, a 5-min maximum intensity (I_{max-5}, mm h^{-1}) and a 5-min weighted rainfall intensity (I_{wt-5}, mm h^{-1}). The 5-min weighted average intensities were calculated by multiplying the 5-min unweighted rainfall intensity averages (I_5, mm h^{-1}) by the rain depth in those 5 min (P_{g-5}, mm), taking the sum of those values and dividing by the total event rain depth (P_g , mm) to give average values that were reflective of the conditions during rainfall:

$$I_{wt-5} = \sum_i^n I_{5,i} \cdot P_{g-5,i} \cdot P_g^{-1} \quad \text{Eq. 2.3}$$

Mean weighted 5-min wind speed, $u_{a,wt-5}$ was also calculated by substituting $I_{5,i}$ with the mean 5-min wind speed, v_{a-5}:

$$u_{a,wt-5} = \sum_i^n v_{a-5,i} \cdot P_{g-5,i} \cdot P_g^{-1} \quad \text{Eq. 2.4}$$

Rainfall inclination angles were calculated using the measured rainfall intensity and wind speed data in conjunction with the relationships between drop size and terminal velocity (see Herwitz & Slye, 1995). Drop size may be estimated using the best-fit equation of Laws and Parsons (1943):

$$D = 2.23 \cdot (0.03937 \cdot I)^{0.102} \quad \text{Eq. 2.5}$$

where D is the median raindrop diameter (mm) and I represents the rainfall intensity (mm h^{-1}).

Drop size diameter (mm) is then used in the following empirical best-fit equation of Gunn & Kinzer (1949) to estimate terminal velocity (U_v, m s^{-1}), which in turn is used to calculate the rainfall inclination angle (P_{inc}, degrees from vertical):

$$U_v = \{3.378 \cdot [\ln(D)]\} + 4.213 \quad \text{Eq. 2.6}$$

$$\tan P_{inc} = v_a \cdot {U_v}^{-1} \quad \text{Eq. 2.7}$$

with P_{inc} also weighted in the same way as I and v_a using Eq. 2.3 and 2.4 to yield an average weighted 5-min rainfall inclination angle, $P_{in,wt-5}$. The meteorological variables that were evaluated against S_F production during this study, including their units, are summarized in Table 2.3.

Table 2.3: Listing of the measured and derived meteorological variables – including their abbreviations and units - that were evaluated against S_F production form the ponderosa pine study trees.

Meteorological Variable	Abbreviation	Unit
Rainfall Depth	P_g	mm
Event Duration	D_E	h
Intra-storm Break Duration	D_B	h
Rain Duration	D_R	h
Maximum 5-min Rainfall Intensity	$I_{max\text{-}5}$	mm h^{-1}
Weighted 5-min Rainfall Intensity	I_{wt-5}	mm h^{-1}
Weighted 5-min Wind Speed	$u_{a,wt-5}$	m s^{-1}
Weighted 5-min Rainfall Inclination Angle	$P_{in,wt-5}$	Degrees (°) from horizontal
Vapour Pressure Deficit	V_{PD}	kPa
Evaporation Coefficient	E	kPa m s^{-1}

2.2.5 Stemflow Metrics

In addition to stemflow volume (S_{Fv}, L), stemflow as a percentage of rainfall on a P_{CA} basis ($S_F\%$); the stemflow funneling ratio (F, dimensionless) were derived for each of the 12 trees at the rain event and study period time scale using equations 2.8 and 2.9, respectively:

$$S_{F\%} = \left[S_{Fv} \cdot \left(P_g \cdot P_{CA}\right)^{-1}\right] \cdot 100\% \quad \text{Eq. 2.8}$$

$$F = S_{Fv} \cdot \left(P_g \cdot B_A\right)^{-1} \quad \text{Eq. 2.9}$$

where P_g is the event or study period rainfall depth (mm) and B_A is the tree basal area (m^2).

The mean depth of rainfall required for S_F initiation ($P_g^{"}$, mm) and the mean rate of S_F flow once S_F commences on a per mm of rainfall basis (Q_{SF}, L mm^{-1}) was estimated empirically for each tree:

$$P_g^{"} = |b \cdot a^{-1}| \quad \text{Eq. 2.10}$$

and Q_{SF} as:

$$Q_{SF} = a \quad \text{Eq. 2.11}$$

where a is the slope and b the intercept of the of S_{Fv} versus P_g linear regression, i.e. $S_{Fv} = a \cdot P_g + b$.

Equations 2.9 and 2.10 can be incorporated into the linear regression of S_{Fv} versus P_g yielding the following equations relating S_{Fv} to P_g, $P_g^{"}$, and Q_{SF}:

$$S_{Fv} = 0, \qquad P_g < P_g^{"} \quad \text{Eq. 2.12}$$

and

$$S_{Fv} = \left(P_g - P_g^{"}\right) \cdot Q_{SF}\,, \qquad P_g \geq P_g^{"} \quad \text{Eq. 2.13}$$

Both $P_g^{"}$ and Q_{SF} for each tree were divided by P_{CA} to yield two metrics relating to the canopy's per unit area storage effectiveness ($P_{g-PCA}^{"}$, mm m^{-2}) and flow generation efficiency (Q_{SF-PCA}, L mm^{-1} m^{-2}).

2.2.6 Analysis of Tree Traits and Meteorological variables influencing stemflow production

The influence of tree traits and during rain event meteorological variables on S_F production by trees in this study followed the stepwise multiple regression analysis approach of other studies evaluating the impact these biotic and abiotic factors have on S_F yield (Van Stan et al.,

2014; McKee and Carlyle-Moses, 2017; Santos Terra, 2018; González-Martínez et al, 2022). Specifically, stepwise-up multiple regression analysis was conducted with S_{Fv} as the dependant variable and P_g and other meteorological factors (see Table 2.3) as the independent variables for each tree. Events included in the analysis were all those greater than or equal to the smallest P_g depth that generated S_F, even if subsequent larger P_g events did not produce S_F (see Carlyle-Moses and Schooling, 2015). In all instances in which multiple regression was used, the relationships between the independent variable and the dependent variable were evaluated and where justified data transformations (e.g., x^2, x^3, ln(x), x^{-1} or $\sqrt{x}$) were made to improve linearity. Multicollinearity among independent variables was assessed using the criterion of $R^2 < 0.64$ (Hair et al., 1998).

2.2.7 Stemflow Infiltration Areas

During the summer of 2022, S_F was simulated on 12 additional trees with similar D_{BH} values to the trees used to measure actual S_F the year before. Different trees were selected for the simulation exercise than those used for measuring actual S_F as the ground around the latter trees was disturbed by S_F reservoir placement and foot traffic during S_F and tree trait measurements. Care was taken to minimize any disturbance to the soils proximal to the boles of trees used for the S_F simulation exercise. The S_F simulation methodology of this study followed closely the methods of Llorens et al. (2022) in which simulated dye coloured S_F at a known flow rate was applied to the boles of trees with I_T being derived as the area of ground cover stained by the dye after each simulation run. Specifically, for each tree used for S_F simulation, a PVC flexible plastic tube with 2-mm diameter holes every 3–5 cm and was installed around the circumference at a height of 0.5 – 0.8 m above the ground. A cloth encircling the tree was affixed between the PVC tube and the tree bole and extended approximately 0.15 m below the tube. The cloth captured simulated S_F being released from the holes in the tube and distributed it more evenly along the surface of the tree bole below. The tube encircling the tree was connected to a 12-L container that was suspended from a 2 m step ladder, with the base of the container being approximately 1.5 m above the ground. This resulted in a gravity-fed flow of water from the 12-L container to the tree bole with flow volumes regulated by either using a 0.8-cm or 0.5-cm diameter tube and by increasing or

decreasing the number of exposed holes in the tube encircling the bole. Holes that were closed were done so using concentrated rubber adhesive tape. Flow rate tests with simulated S_F being directly fed into a collection reservoir (where volumes were measured at given time intervals) were conducted to establish the relationship between flow rate and the combination of tube diameter and number of exposed holes in the tube encircling the tree. Once flow rates had been established through tube diameter and hole exposure selection, 5-L of water was mixed with Fluorescent FLT green formulated version of Xanthene dye from Bright Dyes™ (Division of Kingscote Chemicals, Miamisburg, OH, USA) at a concentration of 5 g L^{-1}. This number was determined by emulating the methods of Llorens et al. (2022) where that concentration was used. The simulated S_F flow rates, (S_{Fr}, L h^{-1}) selected were done so to approximate those S_{Fr} rates calculated from trees of similar D_{BH} during the field season the year prior using the following equation:

$$S_{Fr} = Q_{SF} \cdot I_{wt-5} \qquad \text{Eq. 2.14}$$

Before each S_F simulation run, to establish a clear relationship between I_t and soil surface K_{sat}, litterfall was carefully cleared within a 0.4 m area around the tree bole and 4 – 12 L of un-dyed water was slowly applied to the area to thoroughly wet the soil (Schwärzel et al., 2012; Llorens et al., 2022). During the simulation runs care was made to note which areas of the soil were wetted and dye-stained by simulated S_F that dripped from the bole rather than flow to the soil surface directly. Once a S_F simulation run was completed, the visible I_t was measured by breaking the area into rectangles small enough to be measured by a 30 cm ruler, then area was taken by multiplying the length and width of each rectangle and taking the sum.

2.3 Results

2.3.1 Rainfall and During-Event Meteorological Characteristics

Rainfall and associated S_{Fv} were measured from April 15 to November 15, 2021, inclusive as this period was characterized as having P_g fall continuously in the form of rain; being bounded by a mixed rain-snow event on April 10 and a snow event on November 18. During the period of April 15 to November 15 a total of 51 discreet P_g events ≥ 0.2 mm were recorded by the weighing precipitation gauge with a total depth of 117.2 mm. Linear regression

analysis between the weighing precipitation gauge (dependant variable) and the manually read gauge situated at the TRU-Wx meteorological station site (Gauge S-1) found that the slope was significantly less than unity (0.956±0.010, p <0.01) and the y-intercept was significantly less than zero (-0.116±0.043, p <0.01) suggesting that the weighing precipitation gauge underestimated cumulative and individual event P_g depths. A similar analysis was conducted among all the manually read gauges with significant ($p < 0.05$) differences found between the slopes and or y-intercepts of certain gauge pairings. As such, an inverse distance weighting approach with weights proportional to distance squared (see Dingman, 2015) was utilized using the 5 manually read gauges to estimate event and cumulative P_g depths at the location of each of the 12 ponderosa pine trees in which stemflow was measured. Individual P_g event depth and cumulative P_g depth data for each of the 12 trees in which S_{Fv} was measured are found in Appendix B. Mean cumulative P_g from April 15 – November 15 at the study tree locations was 128.7±1.1 mm, $p = 0.05$, and ranged from 125.5 mm at tree M-6 to 131.3 mm at tree M-3. Individual P_g events ranged from an average of 0.2 mm (five instances) to an average of 22.3±0.3 mm, $p = 0.05$, while mean P_g depth for the study period at all trees was 2.5 mm with a distribution that was highly skewed to the right with 47 P_g events (86.3%) having average depths < 4.0 mm and only 2 P_g events (3.9%) with average depths > 10.0 mm. Average event P_g and associated during-event meteorological characteristics are provided in Table 2.4.

Table 2.4: Mean rainfall depth, P_g (mm) and associated meteorological characteristics for each storm

Event # and Date	P_g (mm)	D_E (h)	D_B (h)	D_R (h)	$I_{max\text{-}5}$ (mm h^{-1})	I_{wt-5} (mm h^{-1})	$u_{a,wt5}$ (m s^{-1})	P_{inc} (°)	V_{PD} (kPa)	E (kPa m s^{-1})
01 - Apr 29	2.1	8.08	6.50	1.58	1.3	0.7	0.8	8	0.00	0.00
02 - May 12	2.2	3.92	0.67	3.25	1.3	0.8	0.3	3	0.05	0.02
03 - May 24	2.2	15.67	14.67	1.00	5.0	1.9	0.6	7	0.22	0.19
04 - Jun 05	1.9	15.67	15.33	0.33	5.7	3.4	1.4	13	0.68	0.97
05 - Jun 07	1.7	3.17	2.50	0.67	2.7	1.9	0.7	7	0.05	0.04
06 - Jun 08	2.0	8.83	7.08	1.75	3.2	1.8	0.7	6	0.17	0.16
07 - Jun 10	2.3	3.67	3.17	0.50	7.7	5.9	2.1	18	1.14	1.27
08 - Jun 13	1.3	5.33	4.58	0.75	1.7	1.4	1.8	17	0.04	0.07
09 - Jun 19	3.2	1.17	0.00	1.17	6.4	5.0	1.3	12	0.01	0.02
10 - Jul 01	2.8	3.67	2.92	0.75	11.2	8.5	1.4	13	1.04	2.39
11 - Jul 07	1.3	0.75	0.00	0.75	7.8	6.1	2.1	16	0.29	0.50
12 - Aug 01	3.5	2.75	2.00	2.75	4.9	2.8	1.1	10	0.03	0.07
13 - Aug 16	22.3	16.17	5.33	10.84	40.5	11.5	1.6	14	0.00	0.00
14 - Aug 22	2.3	6.17	4.42	1.75	2.6	1.4	1.3	12	0.07	0.14
15 - Aug 31	5.0	2.08	0.00	2.08	5.3	3.1	1.6	15	0.01	0.01
16 - Sep 04	2.0	6.83	1.50	5.33	2.4	1.6	0.2	2	0.11	0.02
17 - Sep 14	2.5	2.58	0.00	2.58	2.6	1.5	1.7	16	0.03	0.06
18 - Sep 15	7.4	3.25	0.00	3.25	13.6	6.0	0.7	6	0.00	0.00
19 - Sep 17	4.5	17.67	11.5	6.17	2.6	1.2	1.6	16	0.03	0.05
20 - Sep 19	3.9	8.58	6.00	2.58	4.8	0.5	0.7	7	0.13	0.14
21 - Sep 30	2.0	1.92	0.92	1.00	3.4	2.3	2.6	23	0.03	0.08
22 - Oct 10	2.8	1.42	0.00	1.42	5.2	2.8	2.3	21	0.02	0.05
23 - Oct 24	2.5	2.58	0.75	1.83	3.0	2.0	1.5	14	0.22	0.51
24 - Oct 28	11.9	15.67	1.75	13.92	2.5	1.3	0.3	3	0.00	0.00
25 - Oct 29	1.3	2.92	0.50	2.42	1.2	0.9	0.9	9	0.00	0.00
26 - Nov 03	1.7	6.50	4.42	2.08	2.7	1.5	1.6	15	0.00	0.00
27 - Nov 04	2.8	13.75	9.93	4.42	2.2	1.4	1.0	9	0.00	0.00
28 - Nov 05	1.7	0.25	0.00	0.25	13.6	11.3	3.2	26	0.05	0.25
29 - Nov 13	3.0	4.75	0.50	4.25	1.3	1.0	2.1	20	0.00	0.00
30 - Nov 14	4.3	11.42	4.83	6.58	2.5	0.7	0.4	6	0.00	0.00
31 - Nov 15	7.6	3.00	1.58	1.42	12.1	7.6	4.6	33	0.10	0.30
Average	3.8	6.46	3.66	2.88	5.9	3.2	1.4	13	0.15	0.24

2.3.2 Stemflow Volume as a Function of Rainfall

No $S_{Fv} \geq 0.01$ L was generated by any tree for any P_g event < 1.3 mm (20 events). Table 2.5 provides S_{Fv} for each tree during each of the rain events in Table 2.4. Stemflow volume data were not available for two events for Tree M-1 (Event #'s 22 and 23 in Table 2.5) due to the S_F collection tube of that tree becoming dislodged from the collection reservoir prior to the measurement of S_{Fv} and potentially before or during the P_g event. Stemflow volumes ranged from the minimum threshold of 0.01 L (four instances) to 17.37 L for Tree M-8 for Event # 13 (see Figure 2.5 for M-8 maximum). P_g for this storm was 21.9 mm at Tree M-8. The relationship between S_{Fv} and P_g was found to be linear for each tree with a mean R^2 across all trees of 0.741±0.114, ranging from 0.480 for Tree M-1 to 0.921 for Tree M-7 (Table 2.6).

Using the linear regression equation for S_{Fv} versus P_g for Tree M-1 in Table 2.4 and the P_g depth at that tree for those two events, S_{Fv} was estimated to be approximately 0.24 and 0.28 L for Event # 22 and #23, respectively. Taking these two estimated S_{Fv}values for Tree M-1 into consideration, cumulative S_{Fv} across all rain events for all 12 trees during the study period averaged 23.59±19.25 L and ranged from 3.19 L for Tree M-4 to 72.07 L for Tree M-8.

Figure 2.5: Maximum S_{Fv} obtained by Tree M-8 during a storm of 21.9 mm

Using the slope and intercept values of the relationship between S_{Fv} and P_g in Table 2.6, Eqs. 2.10 and 2.11 were used to determine the threshold P_g depth (mm) for S_F generation, $P_g^{''}$, and the mean S_F flow rate (L mm^{-1}) once that threshold had been satisfied, Q_{SF}, for each of the 12 trees. Mean $P_g^{''}$ was 1.9±0.4 mm, ranging from 1.3 mm for Tree M-1 to 2.3 mm for Tree M-12, while Q_{SF} averaged 0.388±0.290 L mm^{-1} and ranged from 0.054 L mm^{-1} for Tree M-4 to

0.963 L mm^{-1} for Tree M-7. Step-forward multiple regression analysis with the $P_g^{''}$ and Q_{SF} values for each of the 12 trees as the dependent variables and the tree characteristics listed in Table 2.1 as the independent variables found that those trees with relatively low average branching angles, A_B (°) and larger diameters, D_{BH}, required a greater P_g threshold for S_F generation, while Q_{SF} values were greater once that threshold P_g was met for trees with greater canopy projection areas, P_{CA}(m^2) and relatively high branching angles.

Table 2.5: Stemflow volume (L) produced by each of the 12 study trees for each precipitation event listed in Table 2.4.

Event #	P_g (mm)	M-1	M-2	M-3	M-4	M-5	M-6	M-7	M-8	M-9	M-10	M-11	M-12
1	2.1	-	-	-	-	2.00	-	-	-	-	-	-	-
2	2.2	-	-	-	-	-	-	-	-	-	-	-	-
3	2.2	-	-	-	-	-	-	-	-	-	-	-	-
4	1.9	-	-	-	-	-	-	-	-	-	-	-	-
5	1.7	-	-	-	-	-	-	-	-	-	-	-	-
6	2.0	-	-	-	-	-	-	-	-	-	-	-	-
7	2.3	0.01	-	0.01	-	0.11	-	-	-	-	-	-	-
8	1.3	-	-	-	-	-	-	-	-	-	-	-	-
9	3.2	0.33	-	0.07	-	0.15	0.06	0.04	0.45	-	-	-	-
10	2.8	-	-	-	-	-	-	-	-	-	-	-	-
11	1.3	-	-	-	-	-	-	-	-	-	-	-	-
12	3.5	0.24	-	0.07	-	0.10	0.09	0.06	0.77	-	-	-	-
13	22.3	3.84	1.53	3.60	1.01	10.48	8.17	9.49	17.37	1.37	8.08	16.08	12.65
14	2.3	-	-	-	-	-	-	-	-	-	-	-	-
15	5.0	1.30	0.17	0.34	0.09	0.64	1.39	0.77	2.05	-	1.10	0.96	0.57
16	2.0	-	-	-	-	-	-	-	-	-	-	-	-
17	2.5	0.18	-	-	-	0.08	-	-	-	-	-	-	-
18	7.4	1.90	0.15	0.97	0.30	1.32	2.85	2.05	5.28	0.29	0.62	2.12	1.80
19	4.5	0.49	-	0.11	-	0.54	0.54	0.44	2.24	-	0.05	-	0.12
20	3.9	0.36	-	0.21	-	0.27	0.19	0.16	1.01	-	-	-	-
21	2.0	-	-	-	-	0.13	-	-	-	-	-	-	-
22	2.8	n.a.	-	0.19	-	0.43	0.55	0.33	1.28	0.03	0.29	0.14	0.13
23	2.5	n.a.	-	-	-	-	-	-	-	-	-	-	-
24	11.9	0.12	0.25	1.48	0.39	2.08	5.44	3.38	11.05	0.76	3.02	5.05	2.79
25	1.3	-	-	0.04		0.07	0.14	0.11	0.24	-	-	-	-
26	1.7	-	-	-	-	-	-	-	0.03	-	-	-	-
27	2.8	-	-	0.30	0.01	0.68	0.65	0.47	2.21	-	0.12	0.09	0.07
28	1.7	1.16	0.11	1.04	0.09	1.71	1.23	0.78	5.84	0.04	2.46	1.77	1.28
29	3.0	-	-	-	-	0.53	0.41	0.46	2.27	-	0.04	-	0.01
30	4.3	-	0.02	0.81	0.15	0.93	2.26	1.45	4.65	0.25	0.91	2.38	1.34
31	7.6	4.5	1.16	3.39	1.15	3.85	6.07	4.42	15.33	1.32	7.97	11.00	7.20
Sum	118.0	14.95*	3.39	12.63	3.19	26.10	30.04	24.41	72.07	4.06	24.66	39.59	27.96

* Sum of S_{Fv} from Tree M-1 based on derived S_{Fv} values for events 22 and 23 of 0.24 L and 0.28 L, respectively, derived using linear regression relationship between S_{Fv} and P_g for this tree (see table 2.6).

Table 2.6: Linear regression components of stemflow volume S_{Fv} (L) as a function of event P_g depth (mm) for each of the 12 trees used in this study.

Tree #	Slope	Intercept	R^2	*n*	Standard Error of Estimate (L)
M-1	0.189	-0.241	0.480	26	0.86
M-2	0.071	-0.170	0.739	28	0.18
M-3	0.182	-0.301	0.706	31	0.49
M-4	0.054	-0.110	0.662	28	0.17
M-5	0.447	-0.821	0.814	31	0.87
M-6	0.459	-0.738	0.827	31	0.85
M-7	0.442	-0.904	0.921	31	0.55
M-8	0.963	-1.381	0.752	31	2.26
M-9	0.074	-0.163	0.751	28	0.19
M-10	0.407	-0.769	0.627	28	1.34
M-11	0.777	-1.739	0.794	28	1.70
M-12	0.585	-1.372	0.818	28	1.18

$$P_g^{''} = -0.016A_B + 0.020D_{BH} + 2.05 \qquad R^2 = 0.646,\ n = 12,\ SEE = 0.23 \qquad \text{Eq. 2.15}$$

$$Q_{SF} = 0.028P_{CA} + 0.010A_B - 0.170 \qquad R^2 = 0.755,\ n = 12,\ SEE = 0.16 \qquad \text{Eq. 2.16}$$

Substituting Eqs. 2.15 and 2.16 into Eq. 2.13 yields the following equation for estimating S_{Fv} (L) as a function of P_g depth (mm) for the Ponderosa pine trees at my study site for $P_g \geq P_g^{''}$:

$$S_{Fv} = \left[P_g - (-0.016A_B + 0.020D_{BH} + 2.05)\right] \cdot (0.028P_{CA} + 0.010A_B - 0.170) \qquad \text{Eq. 2.17}$$

and, as per Eq. 2.14, when $P_g < P_g^{''}$, $S_{Fv} = 0$.

2.3.3 Influence of During-Event Meteorological Characteristics on Stemflow Volume

In addition to P_g depth, other storm event meteorological variables were assessed to determine what, if any, influence they had on S_{Fv} from the 12 trees included in this study. Stepwise forward multiple regression following the procedure outlined in section 2.2.6 was used with P_g depth included as the primary independent variable in each regression run to

determine the compounding influence, if any, of the other during-event meteorological variables on individual tree S_{Fv}. Multicollinearity was found between P_g and maximum 5-minute rainfall intensity, $I_{max\text{-}5}$, between the 5-minuted weighted wind speed, $u_{a,wt5}$, and rainfall inclination angle, P_{inc}, and between vapour pressure deficit, V_{PD}, and the evaporation coefficient, E. As such, we excluded $I_{max\text{-}5}$ from the regression analysis since P_g is the primary meteorological factor influencing S_{Fv}. Additionally, $u_{a,wt5}$ and V_{PD} were omitted from the analysis since the influence these variables have on the quantity of S_{Fv} has been shown to be directly related to P_{inc}, in the case of $u_{a,wt5}$, and to E, in the case of both $u_{a,wt5}$ and V_{PD} (see Levia et al., 2011; Van Stan et al., 2011; Carlyle-Moses and Schooling, 2015). Multiple regression was thus conducted with S_{Fv} as the dependent variable, P_g as the primary independent variable and total event duration, D_E (h), storm break duration, D_B (h), rain duration, D_R (h), 5-minute weighted rainfall intensity, I_{wt-5} (mm h^{-1}), rainfall inclination angle, P_{inc} (^{o}), and the evaporation coefficient, E (kPa m s^{-1}), for the storm event as potential secondary independent variables. The results of the regression analysis are found in Table 2.7.

Rainfall inclination angle, P_{inc}, was found to have a significant ($p \leq 0.05$) positive correlation with S_{Fv} for all trees except Tree M-5, although P_{inc} was significant for Tree M-5 at the $p = 0.069$ level when included with P_g and D_R. Rainfall duration, D_R, was significant ($p \leq 0.05$) for 3 of the 12 trees (25%), while the evaporation coefficient was only significant ($p \leq 0.05$) for 1 of the 12 trees (8%).

Table 2.7: Multiple regression components of stemflow volume S_{Fv} (L) as a function of event P_g depth (mm) and other significant ($p \leq 0.05$) meteorological variables for each of the 12 trees used in this study.

Tree #	P_g (mm)	P_{inc} (°)	D_R (h)	E (kPa m s^{-1})	Intercept	R^2	Adjusted R^2	n	Standard Error of Estimate (L)
M-1	0.295	0.050	-0.204	-0.395	-0.563	0.812	0.776	26	0.55
M-2	0.087	0.011	-0.032	-	-0.277	0.871	0.855	28	0.14
M-3	0.183	0.041	-	-	-0.834	0.811	0.797	31	0.41
M-4	0.054	0.012	-	-	-0.266	0.762	0.743	28	0.15
M-5	0.562	-	-0.201	-	-0.670	0.856	0.845	31	0.78
M-6	0.461	0.051	-	-	-1.399	0.860	0.850	31	0.78
M-7	0.442	0.042	-	-	-1.443	0.945	0.942	31	0.46
M-8	0.969	0.179	-	-	-3.699	0.833	0.821	31	1.89
M-9	0.074	0.011	-	-	-0.304	0.801	0.785	28	0.17
M-10	0.408	0.118	-	-	-2.265	0.789	0.789	28	1.03
M-11	0.779	0.135	-	-	-3.451	0.867	0.856	28	1.39
M-12	0.585	0.093	-	-	-2.557	0.881	0.872	28	0.97

2.3.4 Stemflow % and Funnelling Ratios

Table 2.8 provides the mean, median, minimum, and maximum stemflow percentage of event-scale precipitation, S_F% for each of the 12 trees in the study across three P_g depth classes: < 2, 2 – 5, and ≥5 mm. Although the median S_F% for P_g events < 2mm was 0% across all trees, maximum values were high, especially for smaller trees. For example, trees M-3, M-5, and M-8 had maximum S_F% that exceeded 20% and, in the case of M-1, exceeded 30% of P_g for this P_g depth class. Large maximum S_F% values are also found for certain trees in the two other P_g depth classes, including 20.3% for tree M-5 in the 2 – 5mm P_g depth class and 31.3% for tree M-1 in the ≥5 mm P_g depth class. Not surprisingly, the large maximum S_F% values translated into high stemflow funneling ratios *F*, including a value of 340.6 for tree M-1 in the <2mm P_g depth class (Table 2.9).

Table 2.8: Stemflow as a percentage of P_g depth (mm) on a per projected canopy area with P_{CA} basis for three P_g depth classes (< 2mm, 2 – 5mm, and ≥5mm) for each of the 12 study trees.

P_g Depth Class (mm)		M-1	M-2	M-3	M-4	M-5	M-6	M-7	M-8	M-9	M-10	M-11	M-12
< 2	Mean	4.3	0.2	3.3	0.1	3.3	2.2	0.8	2.8	0.0	1.7	0.7	0.7
	Median	0.0	0.0	0.0	0.0	0.0	0.0	0.0	0.0	0.0	0.0	0.0	0.0
	Min.	0.0	0.0	0.0	0.0	0.0	0.0	0.0	0.0	0.0	0.0	0.0	0.0
	Max.	33.8	1.7	22.3	0.9	25.5	15.6	5.7	21.6	0.2	12.1	4.9	4.8
2 - 5	Mean	1.4	0.0	0.8	0.0	2.6	1.3	0.8	1.5	0.0	0.2	0.2	0.1
	Median	0.0	0.0	0.0	0.0	0.8	0.0	0.0	0.0	0.0	0.0	0.0	0.0
	Min.	0.0	0.0	0.0	0.0	0.0	0.0	0.0	0.0	0.0	0.0	0.0	0.0
	Max.	5.5	0.1	5.9	0.7	20.3	9.6	4.7	6.9	0.5	1.6	2.4	1.8
≥5	Mean	13.9	1.4	5.0	0.9	5.8	8.4	4.2	6.6	0.5	2.5	2.2	2.1
	Median	13.8	0.8	4.0	0.7	3.7	6.8	4.0	5.3	0.4	1.8	1.5	1.4
	Min.	0.5	0.0	0.8	0.0	2.6	5.1	1.3	2.9	0.0	0.1	0.0	0.2
	Max.	31.3	4.2	13.7	2.8	11.6	15.5	7.9	13.6	1.4	8.1	6.3	5.6

Table 2.9: Stemflow funnelling ratios, F (dimensionless) for three P_g depth classes (< 2mm, 2 – 5mm, and ≥5mm) for each of the 12 study trees.

P_g Depth Class (mm)		M-1	M-2	M-3	M-4	M-5	M-6	M-7	M-8	M-9	M-10	M-11	M-12
< 2	Mean	42.9	2.6	19.9	0.8	13.6	9.1	2.8	16.6	0.1	5.9	3.1	1.9
	Median	0.0	0.0	0.0	0.0	0.0	0.0	0.0	0.0	0.0	0.0	0.0	0.0
	Min.	0.0	0.0	0.0	0.0	0.0	0.0	0.0	0.0	0.0	0.0	0.0	0.0
	Max.	340.6	18.1	133.9	6.6	104.1	64.0	21.1	125.8	0.7	41.2	22.0	13.1
2 - 5	Mean	14.4	0.1	4.9	0.3	10.5	5.2	2.8	8.9	0.1	0.5	0.7	0.3
	Median	0.0	0.0	0.0	0.0	0.8	0.0	0.0	0.0	0.0	0.0	0.0	0.0
	Min.	0.0	0.0	0.0	0.0	0.0	0.0	0.0	0.0	0.0	0.0	0.0	0.0
	Max.	55.7	1.4	35.7	4.9	82.9	39.3	17.6	40.5	2.0	5.4	10.7	5.0
≥5	Mean	139.9	14.7	29.8	6.5	23.6	34.6	15.5	38.2	1.8	8.5	9.9	5.7
	Median	139.4	8.3	23.9	5.2	15.2	27.8	14.7	30.9	1.7	6.0	6.7	3.7
	Min.	5.3	0.0	4.6	0.0	10.4	20.7	5.0	17.0	0.0	0.3	0.0	0.4
	Max.	315.7	44.7	82.3	19.9	47.3	63.3	29.5	79.0	5.4	27.5	28.3	15.3

2.3.5 Stemflow Infiltration Funnelling Ratios

Average during event S_F flow rates, S_{Fr}, on a L h^{-1} basis for each tree and storm event combination in which S_F was produced was estimated by multiplying the stemflow flow rate on a per mm of P_g basis, Q_{SF}, by the average rainfall intensity over the entire storm event, I_{Mean} ($I_{Mean} = P_g / D_E$). These S_{Fr} values were found to vary from a minimum of 0.01 L h^{-1} (Tree M-4, Event #26) to a maximum of 9.60 L h^{-1} (Tree M-8, Event #28). Mean S_{Fr} values for all storms that produced S_F for each tree were divided into three I_{Mean} classes: < 1.0 mm h^{-1}, 1.0 - < 2.0 mm h^{-1}, and ≥ 2.0 mm h^{-1}. The influence of projected canopy area, P_{CA}, and branching angle, A_B, on S_{Fr} is evident. For example, for trees with P_{CA} values < 10 m^2, the

two trees with near horizontal (i.e., 0°) mean A_B values (M-2 and M-4) had a mean S_{Fr} value of 0.26±0.07 L h^{-1} for P_g events with $I_{Mean} \geq 2.0$ mm h^{-1}, which was significantly lower (p = 0.048) than the mean S_{Fr} of 1.28±0.52 L h^{-1} for the same class of I_{Mean} events for those trees with P_{CA} values < 10 m^2 that had inclined branches (36° to 47°, Trees M-1, M-3, M-5, M-6, and M-7). Additionally, S_F volumetric flow rates for those trees with inclined branches (A_B > 20°) were significantly greater (p = 0.023; 2.62±0.86 L h^{-1}) for trees with relatively large P_{CA} values (i.e., ≥ 10 m^2, Trees M-8 through M-12) compared to trees with smaller P_{CA} (1.28±0.52 L h^{-1}) under $I_{Mean} \geq 2.0$ mm conditions.

Using the S_{Fr} values measured during our natural S_F experiments as a guide, simulated S_F was applied to 12 additional trees to determine the S_F infiltration area, I_T (m^2) under differing tree size (D_{BH}) and S_{Fr} scenarios as described in Section 2.27. A total of 29 simulation runs were made. Infiltration area values varied from 5 x 10^{-5} m^2 for a tree with a D_{BH} of 22.9 cm and a simulated S_{Fr} of 0.90 L h^{-1} to 1.53 x 10^{-1} m^2 for a tree having a D_{BH} of 24.1 cm with a simulated S_{Fr} application of 8.31 L h^{-1}. The relationship between I_T and simulated S_{Fr} values was found to be linear (Figure 2.5) taking the form of Eq. 2.18:

$$I_T = 0.0122\, S_{Fr} + 0.002 \quad R^2 = 0.585,\ n = 29,\ SEE = 0.024 \qquad \text{Eq. 2.18}$$

The slope of Eq. 2.34 suggests that I_T increases around the boles of the selected trees at an average rate of 1.22 x 10^{-2} m^2 for every 1 L h^{-1} increase in S_{Fr}. With the relationship between S_{Fr}, I_T, and the saturated hydraulic conductivity of the surface soil, K_{sat}(mm h^{-1}), being $I_T = S_{Fr} \cdot K_{sat}^{-1}$ (see Herwitz, 1986; Levia and Germer, 2015; Carlyle-Moses et al., 2018) this suggests that the mean K_{sat} values around the trees in which simulated S_{Fr} was applied averaged approximately 82 mm h^{-1}.

2.4 Discussion

2.4.1 Stemflow Volume as a Function of Rainfall

Stemflow volume (S_{Fv}) produced by individual ponderosa pine trees in my study was strongly controlled by event rainfall depth (P_g), indicating that rainfall depth is the primary

driver of stemflow generation. This agrees with other studies examining S_{Fv} production (e.g. Sato et al., 2025; Karimi et al., 2026). The strong dependence of S_{Fv} on P_g has been shown at the individual tree-scale (e.g. Van Stan et al., 2014; Carlyle-Moses and Schooling, 2015; de Lima, J. A. et al., 2026) and at the forest stand scale (e.g., Orr et al., 1972; Marin et al., 2000; McKee and Carlyle-Moses, 2017; Lu et al., 2024). A strong correlation between S_{Fv} and P_g was expected, as S_{Fv} is a form of drainage from a tree canopy, with greater P_g inputs resulting in correspondingly greater S_{Fv} drainage outputs. Coefficient of determination (R^2) values associated with S_{Fv} versus P_g linear regressions for the individual ponderosa pine trees in my study averaged 0.741 and ranged from 0.480 for tree M-1 to 0.921 for tree M-7. This indicates that 48 to 92 percent of the variability of S_{Fv} among events at the individual tree-scale is explained by variations in event P_g depth alone. For comparison, Şensoy and Tanyel (2021) found that the R^2 values of the linear relationships between S_{Fv} and P_g for 7 individual trees, each representing different species in northwestern Turkey, ranged from 0.472 for hop hornbeam (*Ostrya carpinifolia*) to 0.905 for holm oak (*Quercus ilex*).

The linear form of the S_{Fv}–P_g relationship likely reflects both the relatively small rainfall depth required to saturate canopy storage (e.g., Carlyle-Moses and Schooling, 2015; Deng et al., 2021; Zhao et al., 2025) and the seemingly proportional increase in stemflow drainage once canopy storage capacity has been met (see Carlyle-Moses and Price, 2006; McKee and Carlyle-Moses, 2017). Once a tree's canopy storage capacity has been filled, the proportion of P_g drained via the tree's branch and bole system as S_{Fv} remains approximately constant. In my study, for $P_g < 1.3$ mm, no $S_{Fv} \geq 0.01$ L was generated, indicating that this is the depth threshold required for Ponderosa pine. My research indicates that at lower rainfall amounts, ponderosa pine's bark water storage capacity exceeds the rainfall rate, as is the case with rough-barked redwood and Douglas-Fir trees (Levia and Germer, 2015). In addition, Norozi et al. (2024) noted that the rougher-barked *Pinus eldarica* produced smaller S_{Fv} than the smoother barked *Cupressus arizonica*.

2.4.2 Influence of During-Event Meteorological Characteristics on Stemflow Volume

In my study, average rainfall intensity ($I_{wt\text{-}5}$) was typically a poor predictor of S_{Fv} relative to P_g. There was only one case (Tree M-1) where the R^2 relating $I_{wt\text{-}5}$ to S_{Fv} (R^2 =

0.57) was greater than the R^2 relating P_g to S_{Fv} ($R^2 = 0.48$) however the combined R^2 with all variables was higher with P_g being the primary independent variable. Some studies have reported that $I_{wt\text{-}5}$ exerts a positive influence upon S_F generation (e.g. Van Stan et al. 2014; Lu et al. 2024). Van Stan et al (2014) reported that $I_{wt\text{-}5}$ affected middling size *L. tulipfera* the most, while it was mostly insignificant on other species or size classes. They suggest that the differences between their study and others may be due to larger trees obscuring the true relationship between $I_{wt\text{-}5}$ and S_F for smaller tree size classes. Others have expressed that $I_{wt\text{-}5}$ exerts a negative influence (e.g. Carlyle-Moses 2004, Levia et al. 2010). Carlyle-Moses (2004) suggests that the larger raindrops and higher speeds associated with intense precipitation result in splashing or dripping from trees. Still others have reported no clear relationship (e.g. Pressland 1973). The reason for the lack of relationship suggested by Pressland (1973) is not stated, however they do note that their study contrasts with Slatyer (1965), who reported a negative relationship. My study demonstrated no relationship between S_{FV} and $I_{wt\text{-}5}$, however rainfall inclination angle (P_{inc}), a variable closely associated with rainfall intensity did have a significant relationship.

Rainfall inclination angle exerted a strong positive influence on S_{Fv}, suggesting that wind-driven rainfall plays an important role in stemflow generation in ponderosa pine. With the exception of Tree M-5, P_{inc} was positively related to S_{Fv} at the 95% confidence level. For Tree M-5, it was related at the 93% confidence level. This positive relationship is similar to that reported in previous research on other species (Van Stan et al. 2011, Carlyle-Moses and Schooling 2015) he latter being particularly important because it was also conducted in a semi-arid environment. Many studies discuss the influence of wind-driven rainfall on S_F processes (e.g. Xiao et al., 2000; André et al., 2008; Staelens et al., 2008; Šraj et al., 2008; Van Stan et al., 2014; Iida et al., 2017; Zabret et al., 2018; Zabret and Šraj, 2019, Zabret and Šraj 2021). Interestingly, lone among these studies, Zabret and Šraj (2021) observed no interaction between wind characteristics and S_F generation. They do state however, that their method could have been improved by taking into account the average data on wind conditions during the event. Van Stan et al. (2014) observed intense, high-wind storms to have a significant positive relationship with S_F yield, and André et al. (2008) found, apart from P_g, wind speed was the only variable with a positive significant relationship to S_{Fv} and S_{Fr}. In my study, event 28 initiated stemflow at the second-lowest P_g ($P_g = 1.7$ mm) and was

characterized by both the highest P_{inc} and the second-highest $I_{wt\text{-}5}$. This storm is unique in that it is the only storm under 7.4 mm depth to produce stemflow from all trees. In contrast, storm event 25 with a P_g depth of only 1.3 mm produced S_F on 5 trees and had a P_{inc} of 9. While it is remarkable that the storm produced S_F at such a low threshold, all meteorological variables were below average. A possibility is that the canopies were still saturated from a previous storm of 11.9 mm $P_{g,}$ considerably above the average of 3.8. There is one other low P_g (1.7 mm) storm of note, (Event 26) which produced S_F from one tree. This rainfall inclination angle for this event was 15, which is higher than the average of 13. With the mean $P_g^{''}$ being 1.9±0.4 mm, it is possible that during storms with depths lower than the threshold, rainfall inclination angle becomes a large factor in determining whether or not trees will produce S_F.

When present, rainfall duration (D_R) exerted a generally negative influence on S_{Fv} in ponderosa pine, suggesting that prolonged rainfall events may reduce stemflow efficiency in smaller trees. For small trees, rainfall of short duration with high $I_{wt\text{-}5}$ may produce more S_{Fv} than rainfall events of long duration with low $I_{wt\text{-}5}$ (Bellot and Escarre, 1998, Staelens et. al 2008).In my study, D_R had a significant negative relationship with S_{Fv} for three trees (M-1, M-2, and M-5), contrasting with much of the previous research that reports positive relationships between D_R and S_{Fv} (e.g., Kuraji et al., 2001; Levia, 2004). Trees M-3 and M-4 exhibited no relationship, which may have been caused by morphological differences. Tree M-4 had very low branching angle (A_B), which likely caused it to produce significantly less S_F than it would have otherwise, and may have contributed to the S_F produced having no relationship with D_R. Previous studies (e.g. Levia et al., 2015) have determined that the number of branches (B_n) positively affects a tree's ability to produce S_F and Tree M-3 had a low B_n for its size. While there are some studies (Siegert and Levia 2014) who found the influence on interception loss by D_R to be negligible upon smooth-barked trees, there are no identified studies that have found D_R to have a negative relationship with S_{Fv}. Since I conducted my study in a semi-arid climate, it is possible that low intensity events over a longer D_R may experience sufficient evaporation to reduce S_{Fv}. Due to the lack of a relationship between ponderosa S_F and E in my study, further research is needed to confirm this assumption.

Evaporation exerted little influence on S_{Fv} in ponderosa pine, suggesting that evaporative losses during rainfall events were generally insufficient to substantially alter stemflow generation. Of the twelve trees, only M-1 had a significant negative relationship between the evaporation coefficient (E) and S_{Fv}. This negative relationship is consistent with the assumptions of Van Stan et al. (2014) regarding *F. grandifolia* and *L. tulipifera*, in which S_F generation was assumed to be reduced by evaporation along the canopy storage-to-drainage pathway. Cayuela et al. (2018) linked increased wind speed and VPD to increased evaporation from their trees. Andre et al (2008) found that while evaporation may increase $P_g^{''}$, evaporation has no significant effect on S_{Fv} for rain events larger than the $P_g^{''}$, since evaporation during rain is very low. The limited significance of E in my study supports this, indicating that, if present, evaporation likely plays a secondary role to S_{FV} relative to other meteorological and structural variables such as P_g, P_{inc}, and branch architecture.

Tree structural characteristics, particularly D_{BH} and A_B, exerted a strong influence on S_{Fv} and $P_g^{''}$ in ponderosa pine. For example, Van Stan and Levia (2010) found that there was a positive correlation between D_{BH} and S_F production for both *F. grandifolia* and *L. tulipifera*. In my study, D_{BH} was significantly positively correlated ($p<0.001$) with T_H, C_V, P_{CA}, B_n, C_H, and B_{RI}, and at the 90% confidence level, $R_{H\text{-}W}$. In my study, Trees with greater D_{BH} and low branching angles relative to the other trees required a greater rainfall for $P_g^{''}$. Once those thresholds were exceeded, trees with larger P_{CA} and higher A_B produced greater stemflow drainage through Q_{SF}. While inefficient at larger rainfall events, trees characterized by smaller D_{BH} and steeper A_B generated proportionally greater stemflow during rainfall events with lower P_g. These findings are consistent with previous research demonstrating the importance of branch architecture for stemflow production. For example, Hildebrandt et al (2007) found that very high A_B in Omani cloud forests contributed greatly to S_{Fv}, and Tonello et al (2021), reported that smaller D_{BH} and highly angled branches on 36 tree species positively influenced S_{Fv}.

2.4.3 Stemflow Percent and Funnelling Ratio

Stemflow efficiency in ponderosa pine generally increased with rainfall depth, although meteorological conditions appeared to influence this relationship among rainfall classes. Since S_F efficiency is directly derived from rainfall amount, it is unsurprising that

mean S_F % at the third rainfall depth class (≥ 5 mm) tended to exceed that of the first depth class (< 2 mm). However, both mean and maximum S_F % were substantially lower in rainfall depth class II (2-5 mm). This difference may be explained by the comparatively low $I_{wt\text{-}5}$, max wind, and gust speeds in depth class II storms. The overall mean S_F % for the season was 2.3%, which is comparable to values reported for *Pinus sylvestris* by both Soulsby et al. (2017) and Kermavnar and Vilhar (2017), who had S_F % values of 1.6 and 2.0, respectively. Conversely, Zabret et al (2018) reported a maximum S_F % of only 0.9 % on *Pinus nigra* while Guo et al. (2026) reported an average of 0.9% on *Pinus bungeana*. To compare with a commonly studied deciduous species, Levia et al. (2015) found an average of 2.4% S_F and a maximum of 5.8% on European Beech saplings.

Two trees exhibited exceptionally high S_F %, potentially indicating that certain morphological characteristics can greatly influence efficiency. Tree M-1 had extremely high S_F % and maximum S_F % relative to the literature. Relative to the other trees in this study, tree M-1 had the greatest mean S_F % as well as maximum S_F % for both the lowest and highest rainfall depth classes. Certain ponderosa pine individuals exhibited exceptionally high stemflow efficiencies, indicating that specific tree structural characteristics can greatly enhance stemflow production during low-depth rainfall events. Among all sampled trees, Tree M-1 consistently generated the highest stemflow percentages (S_F %), producing both the greatest mean and maximum S_F % values for the lowest and highest rainfall depth classes. Tree M-1 also produced the highest overall S_F % observed in the study, reaching 33.8% during a 1.8 mm storm, while its second highest value of 31.3% exceeded that of the next most efficient tree during the same storm by more than 200%. These S_F percentages are extremely high, given that S_F often accounts for approximately 5% of incident rainfall (Llorens et al. 2022). While deciduous trees and shrubs can produce S_F up to 45% of rainfall (Levia and Frost 2003), it is highly unusual for a coniferous stand to be so efficient. Tree M-5 also demonstrated comparatively high S_F efficiency, producing the second-highest mean and maximum S_F % in rainfall depth class I during the same storm event, as well as the highest mean, median, and maximum S_F % in depth class II. The maximum was produced from the storm of 1.8 mm. While M-5 possessed a larger D_{BH} than M-1, it also had the highest A_B among all sampled trees, which may have enhanced its ability to efficiently route

water toward the bole during lower intensity rainfall events, consistent with findings reported by Schooling and Carlyle-Moses (2015).

Lower stemflow efficiencies were associated with trees with low A_B and larger D_{BH}, further supporting the influence of tree morphological characteristics upon S_F %. While tree M-9 had the lowest mean S_F % across all depth classes, it was not unique in producing the minimum overall S_F % of 0.0 %. During rain events < 0.7 mm, no tree produced S_F. Within rainfall depth class II, all trees had a minimum of 0.0%. Within the third rainfall depth class, Trees M-2, M-4, M-9, and M-11 also produced S_F % values of 0.0% during a prolonged, low-intensity storm ranging from 11.7 to 12.0 mm in depth. While they had varying D_{BH}, all except M-11 had A_B < 20 degrees, which potentially limited their ability to route water during low-intensity precipitation. This aligns with previous research, such as Schooling and Carlyle-Moses (2015), who found that, for both single- and multi-leader trees, high A_B was associated with higher S_F production. For the present study, at the 95% confidence level, ~ 70% of the variability in mean S_F % across all trees and depth classes can be attributed to a combination of increasing A_B and decreasing D_{BH}. Similarly, Tonello et al (2021) found that D_{BH} > 20 negatively affected S_F efficiency, however they make no mention of A_B.

Similar to S_F %, Funneling ratio (F) varied with rainfall depth and tree morphology, indicating that both precipitation and tree morphology strongly influenced the efficiency with which ponderosa pine concentrated rainfall toward the bole. Similar to S_F %, F is directly derived from P_g, and thus the mean F observed for rainfall depth class III was greater than that of depth class I. Rainfall depth class II again produced lower than expected values, suggesting that low $I_{wt\text{-}5}$ and wind speed associated with these storms may have reduced F despite higher P_g than depth class I. Funneling ratio is also derived directly from B_A; however, it was found to have a stronger relationship with D_{BH}. Mean F exhibited a significant positive relationship with A_B and a weaker but still significant negative relationship with D_{BH} at the 95% confidence level ($R^2 = 0.58$), indicating that trees with steeper branch angles and smaller trunk diameters were more effective at concentrating precipitation. The overall mean F for the study was 13.8, which compares closely with the mean F value of 11.9 reported for a similarly sparse pine forest in Scotland by Soulsby et al. (2017), as derived by Carlyle-Moses et al. (2018).

Several trees produced very large *F*, showing that certain tree characteristics can greatly enhance rainfall concentration towards the bole for both small and large rainfall events. Four trees generated maximum *F* values greater than 100, with four of the five highest values occurring during the smallest rainfall depth class (<2 mm). Within depth class I, Tree M-1 produced both the highest maximum (340.6) and mean (42.9) *F* values for a 1.7 mm event, highlighting the importance of larger A_B and smaller D_{BH} for large *F* from small-scale rainfall events (e.g. Cayuela et al. 2018, Schooling and Carlyle-Moses 2015). Tree M-1 also produced the highest mean (139.9) and maximum (315.7) *F* values within rainfall depth class III, further highlighting the need for a small D_{BH} and high A_B. Trees M-3, M-5, and M-8 were the only other trees across all depth classes to produce maximum *F* values greater than 100, with values of 133.9, 104.1, and 125.8, respectively. All three trees had $A_B > 35$ degrees, and maximum *F* values were produced by the same storm, which varied in depth from 1.4 mm at Tree M-3 to 1.8 mm at Tree M-8. These *F* values are exceptionally high when compared with those reported for both similar and different species. For example, Spencer and van Meerveld (2016) reported maximum *F* less than 20 on *Tsuga heterophylla* and *Thuja plicata*, while McKee and Carlyle-Moses (2017) had a maximum of 111.7 for *Pinus contorta var. latifolia* with D_{BH} 3.3 cm. This last was produced from a rainfall event of 17.4 mm, suggesting that the equivalent depth around that tree was 2042 mm, or 11170% of the incident precipitation. Comparatively, Tree M-1's maximum *F* suggests that the equivalent depth around that tree was 579 mm for the storm of 1.7 mm, or 34060% of the incident precipitation. According to González-Martínez et al. (2022), funneling ratios > 100 such as these are considered exceptionally high for trees > 10 cm D_{BH}, and even small trees typically produce maximum values of 55-75. The lowest mean and maximum *F* values were observed for Tree M-9, which also consistently produced the lowest amount of S_F. This tree possessed both a relatively large D_{BH} (19.4 cm) and low A_B (18°). Trees M-2 and M-4 similarly exhibited low *F* values despite smaller D_{BH} because of extremely shallow branch angles of 4° and 1°, respectively. Tree M-12 also generated relatively low *F* values and possessed both the largest D_{BH} and a comparatively small A_B (24°). Since A_B is the most influential morphological predictor, it is hardly surprising that even with small D_{BH}, trees M-2 and M-4 had low *F*. Tree M-7, while having a smaller D_{BH} and similar A_B to M-8, generated

significantly smaller *F*. The difference in this tree may lie in its comparatively low P_{CA} which was approximately half that of M-8.

Although several trees in my study produced comparatively low *F*, many still generated values exceeding those typically reported for trees of similar size, suggesting that ponderosa pine can maintain relatively efficient rainfall funneling even among lower-producing trees. While my low production trees produced significantly smaller *F* on average, it is important to note for trees M-9 to 12 that they have D_{BH} larger than 10 cm. Historically, trees this large tend to have $F < 10$ (e.g., Chuyong et al. 2004; Germer et al. 2010), meaning that, with the exception of M-9, they all produced higher-than-average maximum *F* at depth classes I and III. Trees M-5 through M-8 demonstrated even greater funneling efficiency, consistently generating maximum *F* values substantially greater than 10 across all three rainfall depth classes. With the exception of M-7, these trees produced minimum *F* higher than 10 in depth class III. Thus, ponderosa pine trees considered relatively low stemflow producers may still generate funneling ratios that exceed values commonly reported for similarly sized trees, highlighting the capacity of the species to effectively concentrate precipitation in semi-arid environments.

Ponderosa pine efficiently concentrated rainfall toward tree boles under both intense low-magnitude storms and less intense high-magnitude precipitation events. This indicates that ponderosa can effectively redistribute water even under the limited rainfall conditions characteristic of semi-arid environments. Due to the semi-arid nature of the study location, there were only 5 storms in the largest rainfall depth class. The maximum rainfall was 21.9 mm and total rainfall during the study season reached only 117.2 mm. Compared with many previous S_F studies (e.g. Fan et al. 2015; Carlyle-Moses et al. 2018; Cayuela et al. 2018) both the largest rainfall depth class and total seasonal precipitation observed in my study were low. Despite the low rainfall inputs, several ponderosa pine individuals were highly efficient in stemflow production and had exceptionally large *F*, demonstrating the species' ability to effectively concentrate precipitation under water-limited conditions. Because stemflow represents a localized point-source input near the tree bole (e.g. Germer et al. 2010; Levia and Germer 2015), this efficient redistribution of rainfall may play an important role in

enhancing localized infiltration and potentially groundwater recharge in semi-arid landscapes where diffuse infiltration is limited.

2.4.4 Stemflow Infiltration Area

Stemflow infiltration areas (I_t) in my study were highly concentrated near tree boles, suggesting that ponderosa pine S_F infiltrates primarily through localized preferential flow pathways. All measured I_t fell within one order of magnitude of estimated I_t derived from infiltration rates associated with trees of similar D_{BH} to the simulation trees. Of the simulated infiltration areas, 38% were smaller than 0.01 m², 51% were smaller than 0.1 m², and only 7% ranged between 0.1 and 0.2 m², resulting in an average I_t of 0.03 m². This average directly compares with that of Llorens et al. (2022), who reported an average of 0.0288 m^2 despite reporting an average K_{sat} value of 9901 mm h^{-1}. Their minimum of 0.0035 m^2 was larger than mine of .00005 m^2, and their maximum of 0.0951 m^2 (290 Lh^{-1}) was smaller than mine of 0.153 m^2 (8.31 Lh^{-1}). In contrast, Schwärzel et al. (2012) reported a substantially larger infiltration area of 0.245 m² for a single tree with a surface K_{sat} of 415.4 mm h^{-1} and flow rates ranging from 18–150 L h^{-1}. Similar to observations in my study, they discovered that the majority of S_F infiltration into the soil was vertically directed when observed close to the stem before moving laterally farther from the stem along both coarse and fine root pathways (Schwärzel et al. 2012). Although subsurface stemflow pathways were not directly explored in my study, the taproot structure of ponderosa pine may have contributed to the small I_t I observed. Further supporting the idea of highly localized I_t, Tischer et al. (2020) found *Acer pseudoplatanus L.* to have a maximum I_t of 0.03696 m^2 and *Fagus sylvatica L.* a maximum I_t of 0.02002 m^2. They noticed that I_t decreased with increasing soil depth, and S_F inputs were far more concentrated than previously assumed, indicating preferential flow along root systems.

Measured I_t in my study were generally much closer to estimated values than those reported in previous research (e.g. Llorens et al. 2022), suggesting that macropores near ponderosa pine boles may substantially influence infiltration dynamics. In my study, 55% of the measured I_t were in the same order of magnitude as the estimated I_t, and the other 45% were within one order of magnitude. Of the total, 38% of the measured values were one order of magnitude larger, and 7% were one order of magnitude smaller. Interestingly, my results

(with the exception of the 7%) directly contradict those of previous studies such as Metzger et al. (2021), who calculated I_t to generally be two orders of magnitude smaller than estimated. Similarly, Llorens et al. (2022) observed I_t values that were 1-2 orders of magnitude smaller than estimated. One possible explanation for the difference is methodology. These studies relied on the ROSETTA model to estimate K_{sat}. ROSETTA is a modelling approach that excludes the influence of soil macropores, whereas my study measured K_{sat} directly near the boles of trees with similar D_{BH} to the simulation trees. When a major outlier was included, the average K_{sat} of my measured data was 775.2 mm h^{-1} with larger infiltration areas, and the average estimated K_{sat} was 219.7 mm h^{-1} with smaller infiltration areas. Excluding the outlier reduced the average measured K_{sat} to 160 mm h^{-1}. The outlier itself produced an I_t of 0.00005 m^2 from a flow rate of 0.5 L h^{-1} and extrapolated rainfall intensity of 1.25 mm h^{-1}. Following, the measured K_{sat} was 18000 mm h^{-1}. Unique to this tree, there was an approximately 2.5 cm-wide gap between the trunk and the soil (Figure 2.5a), extending to an unknown depth, likely functioning as a direct preferential flow pathway. There is a possibility that, once this pathway ended, S_F spread laterally beneath the surface (e.g., Schwarzel et al. 2012, Friesen 2020). At higher rates, S_F dripped from bark and branches, forming throughfall (T_F). Ordinarily, colouration resulting from this splash effect would be subsequently eliminated from analysis as T_F; however in my study, some splash zones were so close to the bole that they became indistinguishable from I_t (Figure 2.5b).

Figure 2.5 a) Unique gap between tree and soil for outlier b) small infiltration areas resulted in drip becoming indistinguishable from flow

Stemflow, while volumetrically insignificant at the stand level, can represent an important component of incident precipitation. While coniferous species are typically considered inefficient S_F producers, several trees in this study generated comparatively high S_F percentages and exceptionally large F, particularly during low-depth rainfall events. Similarly, Zhang et al. (2021) quantified S_F % across different climate types, noting that in arid areas with minimal precipitation, S_F % was significantly higher than in boreal, warm-temperate, and equatorial climate types. In my study, S_{Fv} was primarily controlled by P_g,

with additional influence from P_{inc} during short, high-intensity events, while tree traits—most notably A_B and D_{BH} —strongly governed S_F % and P_g''. The concentration of S_F into I_t near the base of trees suggests that S_F may act as a point-source input of localized infiltration and groundwater recharge in environments where diffuse infiltration is limited. Given projected increases in evaporative demand and rainfall variability under a changing climate (Van stan and Pinos 2024), the capacity of ponderosa pine to efficiently redistribute precipitation via S_F at relatively low P_g suggests that tree types such as ponderosa may be of increasing importance for the forest water balance and soil moisture dynamics in semi-arid regions (e.g. Martinez-Meza and Whitford 1996)

2.5 Conclusion

My study demonstrates that stemflow in ponderosa pine may provide a significant input to soil moisture despite representing only a small portion of total rainfall. While S_F only accounted on average for only 2.3% of incident precipitation, certain individual trees produced exceptionally high S_F % and F. My findings further demonstrate the importance of S_F study not only at the stand scale, but upon individual trees as well (Van Stan et al., 2014; Carlyle-Moses and Schooling, 2015; Katul et al. 2025). More broadly, my work contributes to a robust body of research (e.g. Pressland 1976; Levia 2004; Carlyle-Moses et al. 2015; Zhang et al 2021), demonstrating that S_F should not be viewed solely as a minor component of the hydrological cycle. Instead, S_F creates infiltration hotspots that influence soil moisture distribution, nutrient cycling, and potentially subsurface recharge. In semi-arid ecosystems where water availability strongly limits ecological processes, these concentrated inputs may be extremely important.

Rainfall depth was found to be the primary factor for S_F production, explaining a large proportion of S_F variability. No measurable stemflow was generated during storms below 1.3 mm rainfall depth. Generally, once a P_g" of approximately 1.9 mm was exceeded, S_F production commenced, however certain storm and tree characteristics could sometimes reduce this threshold. Stemflow production cannot be explained by rainfall depth alone, however. Trees characterized by steeper A_B and smaller D_{BH} produced greater S_F %, larger F, and lower P_g" than trees with shallow A_B and larger D_{BH}. Several meteorological variables

other than P_g were investigated. Rainfall inclination angle consistently enhanced S_F production, highlighting the importance of wind-driven rainfall especially in low-depth rainfall conditions. In contrast, when D_R was influential, it had a negative relationship with S_F, contrary to previous S_F studies (e.g. Levia 2004; Zabret and Šraj 2021; Zhang et al. 2021). Rainfall intensity and E exerted comparatively weak and inconsistent influences on S_{Fv}. My findings suggest that, in semi-arid ponderosa pine stands, the interaction between P_g, P_{inc}, and branching architecture is the most important factor in controlling S_F generation. Perhaps this is an avenue that can be explored in future forest management practices. Branching architecture could be investigated for selective breeding programs to increase stemflow and aid survivability with increasing climate change in semi-arid climates.

The exceptionally high S_F % and F observed in several trees demonstrate that individual trees can efficiently concentrate large magnitudes of rainfall towards their boles even under low or short precipitation events. Mean F averaged 13.8, while maximum event-scale values exceeded 300 for certain trees. These high F values were particularly pronounced for smaller trees with steep A_B, indicating that collective tree structure may strongly influence the spatial redistribution of rainfall within coniferous forests. While research exists that has quantified $S_F I_t$ (e.g. Schwärzel et al. 2012; Carlyle-Moses et al. 2018; Llorens et al. 2022), none identified have been conducted on ponderosa pine. Simulated $S_F I_t$ were consistently small, averaging only 0.03 m² and rarely exceeding 0.15 m². This indicates that on ponderosa pine, S_F infiltrates as a highly localized point-source input. My results support growing research that S_F infiltrates using preferential pathways near tree boles and may potentially lead to groundwater recharge (Hemr et al. 2023; Pinos et al. 2023; Van Stan and Pinos 2024).

As climate change is projected to alter precipitation regimes throughout western North America (Neilsen et al. 2024), understanding how individual trees capture and redistribute rainfall is important. The potential of ponderosa pine to generate S_F under the small storm events characteristic in the type of climate where my study was undertaken suggests that this species may play a role in maintaining localized soil moisture and groundwater inputs during periods of drought (Schooling 2014; Gordon et al. 2020). The findings of my study provide further insight into S_F in semi-arid forests and may provide a

direction for future investigations examining the role of S_F in ecosystem resilience and critical zone processes under a changing climate.

Overall, my study demonstrates that ponderosa pine can efficiently redistribute rainfall through S_F even under the low precipitation conditions of semi-arid environments. While S_F constitutes a relatively small component of precipitation at the stand scale, its strong concentration effect and localized infiltration patterns indicate that it may play an enhanced role in controlling near-stem soil moisture and critical zone hydrology (Carlyle-Moses et al. 2018). Given the projected increases in rainfall variability and evaporative demand associated with climate change, understanding how tree morphology and meteorological conditions govern stemflow generation may become increasingly important for predicting ecohydrological responses in semi-arid forests.

2.6 References

André, F., Jonard, M., & Ponette, Q. (2008). Influence of species and rain event characteristics on stemflow volume in a temperate mixed oak–beech stand. *Hydrological Processes*, *22*(22), 4455–4466. https://doi.org/10.1002/hyp.7048

Bellot, J., & Escarre, A. (1998). Stemflow and throughfall determination in a resprouted mediterranean holm-oak forest. *Annuals of Forest Science, 55*(7), 847–865. https://doi.org/10.1051/forest:19980708

Brown Jr., J. H., & Barker Jr., A. C. (1970). An analysis of throughfall and stemflow in mixed oak stands. *Water Resources Research*, *6*(1), 316–323. https://doi.org/10.1029/WR006i001p00316

Buttle, J. M., Toye, H. J., Greenwood, W. J., & Bialkowski, R. (2014). Stemflow and soil water recharge during rainfall in a red pine chronosequence on the oak ridges moraine, southern Ontario, Canada. *Journal of Hydrology*, *517*, 777–790. https://doi.org/10.1016/j.jhydrol.2014.06.014

Callaham, R. Z. (2013). *Pinus ponderosa: geographic races and subspecies based on morphological variation*. U.S. Department of Agriculture, Forest Service, Pacific Southwest Research Station. https://doi.org/10.2737/psw-rp-265

Carlyle-Moses, D. E. (2004). Throughfall, stemflow, and canopy interception loss fluxes in a semi-arid Sierra Madre Oriental matorral community. *Journal of Arid Environments*, *58*(2), 181–202. https://doi.org/ 10.1016/S0140-1963(03)00125-3

Carlyle-Moses, D.E., Gash, J.H.C. (2011). Rainfall interception loss by forest canopies. In: Levia, D., Carlyle-Moses, D., Tanaka, T. [eds.], *Forest Hydrology and Biogeochemistry*. Ecological Studies, vol 216. Springer, Dordrecht. https://doi.org/10.1007/978-94-007-1363-5_20

Carlyle-Moses, D. E., Iida, S., Germer, S., Llorens, P., Michalzik, B., Nanko, K., Tischer, A., & Levia, D. F. (2018). Expressing stemflow commensurate with its ecohydrological importance. *Advances in Water Resources*, *121*, 472–479. https://doi.org/10.1016/j.advwatres.2018.08.015

Carlyle-Moses, D. E., & Price, A. G. (2006). Growing-season stemflow production within a deciduous forest of southern Ontario. *Hydrological Processes*, 20(17), 3651–3663. https://doi.org/10.1002/hyp.6380

Carlyle-Moses, D. E., & Price, A. G. (2007). Modelling canopy interception loss from a madrean pine-oak stand, northeastern Mexico. *Hydrological Processes*, 21(19), 2572–2580. https://doi.org/10.1002/hyp.6790

Carlyle-Moses, D. E., & Schooling, J. T. (2015). Tree traits and meteorological factors influencing the initiation and rate of stemflow from isolated deciduous trees. *Hydrological Processes*, *29*(18), 4083–4099. https://doi.org/10.1002/hyp.10519

Cayuela, C., Llorens, P., Sánchez-Costa, E., Levia, D. F., & Latron, J. (2018). Effect of biotic and abiotic factors on inter- and intra-event variability in stemflow rates in oak and pine stands in a mediterranean mountain area. *Journal of Hydrology*, *560*, 396–406. https://doi.org/10.1016/j.jhydrol.2018.03.050

Chang, S.-C., & Matzner, E. (2000). The effect of beech stemflow on spatial patterns of soil solution chemistry and seepage fluxes in a mixed beech/oak stand. *Hydrological Processes*, *14*(1), 135–144. https://doi.org/10.1002/(SICI)1099-1085(200001)14:1<135::AID-HYP915>3.0.CO;2-R

Chuyong, G. B., Newbery, D. M., & Songwe, N. C. (2004). Rainfall input, throughfall and stemflow of nutrients in a central African rain forest dominated by ectomycorrhizal trees. *Biogeochemistry*, *67*(1), 73–91. https://doi.org/10.1023/B:BIOG.0000015316.90198.cf

de Lima, J. A., van Stan II, J. T., Lewińska, K., Dradrach, A., Ceglarek, J., & Tonello, K. C. (2026). Stemflow dynamics in the Jamari National Forest (Brazilian Amazon): II. Solute concentrations and flux dynamics. *Biotropica*, *58*(2), e70193. https://doi.org/10.1111/btp.70193

Deng, Y., Ke, J., Wu, S. et al. (2021). Examining the role of throughfall and stemflow on epikarst water recharges using deuterium excess data. *Carbonates Evaporites* 36, 42 https://doi.org/10.1007/s13146-021-00712-x

Durocher, M. G. (1990). Monitoring spatial variability of forest interception. *Hydrological Processes*, *4*(3), 215–229. https://doi.org/10.1002/hyp.3360040303

Fan, J., Oestergaard, K. T., Guyot, A., Jensen, D. G., & Lockington, D. A. (2015). Spatial variability of throughfall and stemflow in an exotic pine plantation of subtropical coastal Australia. *Hydrological Processes*, *29*(5), 793–804. https://doi.org/10.1002/hyp.10193

Friesen, J. (2020). Flow pathways of throughfall and stemflow through the subsurface. In I. I. Van Stan John T., E. Gutmann, & J. Friesen (Eds.), *Precipitation Partitioning by Vegetation: A Global Synthesis* (pp. 215–228). Springer International Publishing. https://doi.org/10.1007/978-3-030-29702-2_13

Fryer, Janet L. 2018. Pinus ponderosa var. Benthamiana, p. P. Var. Ponderosa: ponderosa pine. In: *Fire Effects Information System, [Online]*. U.S. Department of Agriculture, Forest Service, Rocky Mountain Research Station, Missoula Fire Sciences Laboratory (Producer). Available: www.fs.usda.gov/database/feis/plants/tree/pinponp/all.html

Germer, S. (2013). Development of near-surface perched water tables during natural and artificial stemflow generation by babassu palms. *Journal of Hydrology*, *507*, 262–272. https://doi.org/10.1016/j.jhydrol.2013.10.026

Germer, S., Neill, C., Krusche, A. v., & Elsenbeer, H. (2010). Influence of land-use change on near-surface hydrological processes: Undisturbed forest to pasture. *Journal of Hydrology*, *380*(3–4), 473–480. https://doi.org/10.1016/J.JHYDROL.2009.11.022

Germer S, Werther L, Elsenbeer H. (2010). Have we underestimated stemflow? Lessons from an open tropical rainforest. *Journal of Hydrology*, *395*(3–4), 169–79. https://doi.org/10.1016/j.jhydrol.2010.10.022

Gómez, J. A., Vanderlinden, K., Giráldez, J. v, & Fereres, E. (2002). Rainfall concentration under olive trees. *Agricultural Water Management*, *55*(1), 53–70. https://doi.org/10.1016/S0378-3774(01)00181-0

González-Martínez, T. M., Williams-Linera, G., & Holwerda, F. (2017). Understory and small trees contribute importantly to stemflow of a lower montane cloud forest. *Hydrological Processes*, *31*(5), 1174–1183. https://doi.org/10.1002/hyp.11114

González-Martínez, T. M., Williams-Linera, G., & Holwerda, F. (2022). Interactive effects of functional traits and rainfall event size on stemflow in a tropical montane cloud forest. *Ecohydrology*, 15(8), e2466. https://doi.org/10.1002/eco.2466

Gordon, D. A. R., Coenders-Gerrits, M., Sellers, B. A., Sadeghi, S. M. M., & Van Stan II, J. T. (2020). Rainfall interception and redistribution by a common North American understory and pasture forb, *Eupatorium capillifolium* (Lam. dogfennel). *Hydrology and Earth System Sciences*, *24*(9), 4587–4599. https://doi.org/10.5194/hess-24-4587-2020

Guevara-Escobar, A., González-Sosa, E., Véliz-Chávez, C., Ventura-Ramos, E., & Ramos-Salinas, M. (2007). Rainfall interception and distribution patterns of gross precipitation around an isolated Ficus benjamina tree in an urban area. *Journal of Hydrology*, *333*(2–4), 532–541. https://doi.org/10.1016/J.JHYDROL.2006.09.017

Gunn, R., & Kinzer, G. D. (1949). The terminal velocity of fall for water droplets in stagnant air. *Journal of Atmospheric Sciences*, *6*(4), 243–248. https://doi.org/10.1175/1520-0469(1949)006<0243:TTVOFF>2.0.CO;2

Guo, B., Yang, H., Zhu, C. Y., Yan, Z. B., Cao, J. S., & Shen, Y. J. (2026). Rainfall partitioning and interception simulation for typical species in the Taihang Mountains, China. *Agricultural And Forest Meteorology*, *378*. https://doi.org/10.1016/j.agrformet.2025.111004

Hair, J., Anderson, R., Tatham, R., Black, W., (1998). *Multivariate Data Analysis, 5th edition*. Prentice Hall, Upper Saddle River, NJ.

Hemr, O., Vichta, T., Brychtova, M., Kupec, P., Žižlavská, N., Tomášová, G., & Deutscher, J. (2023). Stemflow infiltration hotspots near-tree stems along a soil depth gradient in a mixed oak–beech forest. *European Journal of Forest Research*, 142, 1–16. https://doi.org/10.1007/s10342-023-01592-7

Herwitz, S. R. (1986). Infiltration-excess caused by stemflow in a cyclone-prone tropical rainforest. *Earth Surface Processes and Landforms*, *11*(4), 401–412. https://doi.org/10.1002/esp.3290110406

Herwitz, S. R., & Slye, R. E. (1995). Three-dimensional modeling of canopy tree interception of wind-driven rainfall. *Journal of Hydrology* (Vol. 168, Issue 1). https://doi.org/10.1016/0022-1694(94)02643-P

Hildebrandt, A., al Aufi, M., Amerjeed, M., Shammas, M., & Eltahir, E. A. B. (2007). Ecohydrology of a seasonal cloud forest in Dhofar: 1. Field experiment. *Water Resources Research*, *43*(10). https://doi.org/10.1029/2006WR005261

Honda, E. A., & Durigan, G. (2016). Woody encroachment and its consequences on hydrological processes in the Savannah. *Philosophical Transactions of the Royal Society B: Biological Sciences*, *371*(1703), 20150313. https://doi.org/10.1098/rstb.2015.0313

Iida, S., Levia, D.F., Shimizu, A., Shimizu, T., Tamai, K., Nobuhiro, T., Kabeya, N., Noguchi, S., Sawano, S., Araki, M., (2017). Intrastorm scale rainfall interception dynamics in a mature coniferous forest stand. *Journal of Hydrology*. 548, 770–783. https://doi.org/10.1016/j.jhydrol.2017.03.009.

Johnson, R. C. (1990). The interception, throughfall and stemflow in a forest in highland Scotland and the comparison with other upland forests in the U.K. *Journal of Hydrology*, *118*(1), 281–287. https://doi.org/10.1016/0022-1694(90)90263-W

Johnson, M. S., & Lehmann, J. (2006). Double-funneling of trees: stemflow and root-induced preferential flow. *Écoscience*, *13*(3), 324–333. https://doi.org/10.2980/i1195-6860-13-3-324.1

Johnson, W. M. (1942). The interception of rain and snow by a forest of young ponderosa-pine. *Eos*, *Transactions American Geophysical Union, 23*(2), 566–570. https://doi.org/10.1029/TR023i002p00566

Karimi, K., Attarod, P., Pypker, T. G., Etemad, V., & Pourhashemi, M. (2026). Quantitative and qualitative characteristics of throughfall and stemflow in Quercus brantii and Q. libani forests of the Zagros region, Iran. *Ecohydrology & Hydrobiology*, *26*(1). https://doi.org/10.1016/j.ecohyd.2025.100710

Kermavnar, J., Vilhar, U., (2017). Canopy precipitation interception in urban forests in Relation to stand structure. *Urban Ecosystems*. 20, 1373–1387. https://doi.org/10.1007/s11252-017-0689-7

Kuraji, K., Tanaka, Y., Tanaka, N., & Karakama, I. (2001). Generation of stemflow volume and chemistry in a mature Japanese cypress forest. *Hydrological Processes*, *15*(10), 1967–1978. https://doi.org/10.1002/hyp.250

Laws, J. O., & Parsons, D. A. (1943). The relation of raindrop-size to intensity. *Eos, Transactions American Geophysical Union*, *24*(2), 452–460. https://doi.org/10.1029/TR024i002p00452

Levia Jr, D. F. (2004). Differential winter stemflow generation under contrasting storm conditions in a southern new England broad-leaved deciduous forest. *Hydrological Processes*, *18*(6), 1105–1112. https://doi.org/10.1002/hyp.5512

Levia, D. F., & Frost, E. E. (2003). A review and evaluation of stemflow literature in the hydrologic and biogeochemical cycles of forested and agricultural ecosystems. *Journal of Hydrology*, *274*(1), 1–29. https://doi.org/10.1016/S0022-1694(02)00399-2

Levia, D. F., & Germer, S. (2015). A review of stemflow generation dynamics and stemflow-environment interactions in forests and shrublands. In *Reviews of Geophysics* (Vol. 53, Issue 3, pp. 673–714). Blackwell Publishing Ltd. https://doi.org/10.1002/2015RG000479

Levia, D. F., & Herwitz, S. R. (2002). Winter chemical leaching from deciduous tree branches as a function of branch inclination angle in central Massachusetts. *Hydrological Processes*, *16*(14), 2867–2879. https://doi.org/10.1002/hyp.1077

Levia, D. F., Keim, R. F., Carlyle-Moses, D. E., & Frost, E. E. (2011). Throughfall and stemflow in wooded ecosystems. In D. F. Levia, D. Carlyle-Moses, & T. Tanaka (Eds.), *Forest Hydrology and Biogeochemistry: Synthesis of Past Research and Future Directions* (pp. 425–443). Springer Netherlands. https://doi.org/10.1007/978-94-007-1363-5_21

Levia, D. F., Michalzik, B., Näthe, K., Bischoff, S., Richter, S., & Legates, D. R. (2015). Differential stemflow yield from European beech saplings: The role of individual canopy structure metrics. *Hydrological Processes*, *29*(1), 43–51. https://doi.org/10.1002/hyp.10124

Levia, D. F., Van Stan, J. T., Mage, S. M., & Kelley-Hauske, P. W. (2010). Temporal variability of stemflow volume in a beech-yellow poplar forest in relation to tree species and size. *Journal of Hydrology*, *380*(1–2), 112-120. https://doi.org/10.1016/j.jhydrol.2009.10.028

Levia, D. F., Van Stan, J. T., Siegert, C. M., Inamdar, S. P., Mitchell, M. J., Mage, S. M., & McHale, P. J. (2011). Atmospheric deposition and corresponding variability of stemflow chemistry across temporal scales in a mid-atlantic broadleaved deciduous forest. *Atmospheric Environment*, *45*(18), 3046–3054. https://doi.org/10.1016/j.atmosenv.2011.03.022

Licata, J. A., Pypker, T. G., Weigandt, M., Unsworth, M. H., Gyenge, J. E., Fernández, M. E., Schlichter, T. M., & Bond, B. J. (2011). Decreased rainfall interception balances increased transpiration in exotic ponderosa pine plantations compared with native cypress stands in Patagonia, Argentina. *Ecohydrology*, *4*(1), 83–93. https://doi.org/10.1002/eco.125

Llorens, P., Latron, J., Carlyle-Moses, D. E., Näthe, K., Chang, J. L., Nanko, K., Iida, S., & Levia, D. F. (2022). Stemflow infiltration areas into forest soils around American beech (Fagus grandifolia Ehrh.) Trees. *Ecohydrology*, *15*(2). https://doi.org/10.1002/eco.2369

Lloyd, C. R., & Marques F., A. D. O. (1988). Spatial variability of throughfall and stemflow measurements in Amazonian rainforest. *Agricultural and Forest Meteorology*, *42*(1), 63–73. https://doi.org/10.1016/0168-1923(88)90067-6

Lu, S., Yang, L., Tang, W., Tian, S., Ma, R., Sang, Y., Zhang, J., Zhang, Z., & Shi, Y. (2024). Effects of plantations on rainfall redistribution in a rocky mountain area of north China. *Hydrological Processes*, *38*(10). https://doi.org/10.1002/hyp.15292

Marin, C., Bouten, W., & Sevink, J. (2000). Gross rainfall and its partitioning into throughfall, stemflow and evaporation of intercepted water in four forest ecosystems in western Amazonia. *Journal of Hydrology*, *237*, 40–57. https://doi.org/10.1016/S0022-1694(00)00301-2

Magliano, P., Whitworth-Hulse, J., & Baldi, G. (2019). Interception, throughfall and stemflow partition in drylands: Global synthesis and meta-analysis. *Journal of Hydrology*, *568*, 638–645. https://doi.org/10.1016/j.jhydrol.2018.10.042

Martinez-Meza, E., & Whitford, W. G. (1996). Stemflow, throughfall and channelization of stemflow by roots in three Chihuahuan desert shrubs. *Journal of Arid Environments*, *32*(3), 271–287. https://doi.org/10.1006/jare.1996.0023

Mantovani, V., Terra, M., Ferreira Rodrigues, A., Gomes Cordeiro, N., Mello, J., & de Mello, C. (2022). Biotic and abiotic drivers of stemflow carbon enrichment ratio in tropical trees. *Trees*, *37*, 3. https://doi.org/10.1007/s00468-022-02363-4

McClain, M. E., Boyer, E. W., Dent, C. L., Gergel, S. E., Grimm, N. B., Groffman, P. M., Hart, S. C., Harvey, J. W., Johnston, C. A., Mayorga, E., McDowell, W. H., & Pinay, G. (2003). Biogeochemical hot spots and hot moments at the interface of terrestrial and aquatic ecosystems. *Ecosystems*, *6*(4), 301–312. https://doi.org/10.1007/s10021-003-0161-9

McKee, A. J. (2010). The quantitative importance of stemflow: an evaluation of past research and results from a study in lodgepole pine (pinus contorta var. Latifolia) stands in southern British Columbia. MSc thesis, Thompson Rivers University, Kamloops, British Columbia Canada. 113 p https://arcabc.ca/islandora/object/tru%3A28

McKee, A. J., & Carlyle-Moses, D. E. (2017). Modelling stemflow production by juvenile lodgepole pine (pinus contorta var. Latifolia) trees. *Journal of Forestry Research*, *28*(3), 565–576. https://doi.org/10.1007/s11676-016-0336-9

Meidinger, D., & Pojar, J. (Eds.) (1991). Ecosystems of British Columbia (342 p). *Special Report Series 6*, Victoria, BC: B.C. Ministry of Forests and Range Research Branch. https://www.for.gov.bc.ca/hfd/pubs/docs/srs/srs06.htm

Metzger, J. C., Filipzik, J., Michalzik, B., & Hildebrandt, A. (2021). Stemflow infiltration hotspots create soil microsites near tree stems in an unmanaged mixed beech forest. *Frontiers in Forests and Global Change*, *4*. https://doi.org/10.3389/ffgc.2021.701293

Návar, J. (2011). Stemflow variation in Mexico's northeastern forest communities: its contribution to soil moisture content and aquifer recharge. *Journal of Hydrology*, *408*(1–2), 35–42. https://doi.org/10.1016/j.jhydrol.2011.07.006

Nielsen, M., Cook, B. I., Marvel, K., Ting, M., & Smerdon, J. E. (2024). The changing influence of precipitation on soil moisture drought with warming in the Mediterranean and Western North America. *Earth's Future, 12*, e2023EF003987. https://doi.org/10.1029/2023EF003987

Nicholson, A., E. Hamilton, W.L. Harper, and B.M. Wikeem. (1991) Chapter 8: Bunchgrass Zone. In: D. Meidinger and J. Pojar, [eds.] *Ecosystems of British Columbia*., B.C. Ministry of Forests Research Branch, Victoria B.C.

Norozi, A., Attarod, P., Pypker, T. G., Sadeghi, S. M. M., & Etemad, V. (2024). Estimation of bark water storage capacity of broad- and needle-leaved trees planted in a semi-arid climate zone. *Journal of Arid Environments*, 220, 105100. https://doi.org/10.1016/j.jaridenv.2023.105100

Oliver WW, Ryker RA (1990) Silvics of Ponderosa Pine. In: Burns R.M., Honkala B.H., tech. coords [eds.], *Silvics of North America, Volume 1, Conifers. Agricultural Handbook.* 654. Forest Service, U.S. Department of Agriculture, Washington, DC, pp 413–424.

Orr, H. K., & Rocky Mountain Forest and Range Experiment Station (Fort Collins, Colo.). (1972). *Throughfall and Stemflow Relationships in Second-growth Ponderosa Pine in the Black Hills*. Rocky Mountain Forest and Range Experiment Station, Forest Service, U.S. Department of Agriculture.

Ovington, J. D. (1954). A comparison of rainfall in different woodlands. *Forestry: An International Journal of Forest Research*, *27*(1), 41–53. https://doi.org/10.1093/forestry/27.1.41

Park, A., & Cameron, J. L. (2008). The influence of canopy traits on throughfall and stemflow in five tropical trees growing in a Panamanian plantation. *Forest Ecology and Management*, *255*(5–6), 1915–1925. https://doi.org/10.1016/j.foreco.2007.12.025

Parish, R., Coupé, R., & Lloyd, D. (Eds.). (1996). *Plants of southern interior British Columbia*. Lone Pine.

Pereira, F., Gash, J. H. C., David, J., David, T., Monteiro, P., & Valente, F. (2009). Modelling interception loss from evergreen oak mediterranean Savannas: Application of a tree-based modelling approach. *Agricultural and Forest Meteorology*, *149*, 680–688. https://doi.org/10.1016/j.agrformet.2008.10.014

Petrides, G. A., & Petrides, O. (1998). A Peterson Field Guide to Western Trees: Western United States and Canada. Houghton Mifflin.

Parker, G. G. (1983). Throughfall and stemflow in the forest nutrient cycle. In A. MacFadyen & E. D. Ford (Eds.), *Advances in Ecological Research Volume 13*, 57–133. Academic Press. https://doi.org/10.1016/S0065-2504(08)60108-7

Pinos, J., Latron, J., Levia, D. F., & Llorens, P. (2021). Drivers of the circumferential variation of stemflow inputs on the boles of Pinus sylvestris L. (scots pine). *Ecohydrology*, *14*(8), e2348. https://doi.org/10.1002/eco.2348

Pinos, J., Flury, M., Latron, J., & Llorens, P. (2023). Routing stemflow water through the soil via preferential flow: a dual-labelling approach with artificial tracers. *Hydrology and Earth System Sciences*, *27*(15), 2865–2881. https://doi.org/10.5194/hess-27-2865-2023

Pressland, A. J. (1973). Rainfall partitioning by an arid woodland (Acacia Aneura F. Muell.) in South-Western Queensland. *Australian Journal of Botany*, *21*(2), 235–245. https://doi.org/10.1071/BT9730235

Pressland, A. J. (1976). Soil moisture redistribution as affected by throughfall and stemflow in an arid zone shrub community. *Australian Journal of Botany*, *24*(5), 641–649. https://doi.org/10.1071/BT9760641

Rowe, P. B., & T. M. Hendrix. (1951). Interception of rain and snow by second-growth ponderosa pine. *Eos, Transactions American Geophysical Union*, *32*(6), 903–908. https://doi.org/10.1029/TR032i006p00903

Santos Terra, M. de C. N., de Mello, C. R., de Mello, J. M., de Oliveira, V. A., Nunes, M. H., Silva, V. O., Rodrigues, A. F., & Alves, G. J. (2018). Stemflow in a neotropical forest

remnant: vegetative determinants, spatial distribution and correlation with soil moisture. *Trees*, *32*(1), 323–335. https://doi.org/10.1007/s00468-017-1634-3

Sato, T., Ohosawa, K., Ebata, K., & Matsumoto, Y. (2025). Stemflow measurement on large leaning trees: examination of stem lean effect on stemflow. *Hydrological Processes*, *39*(1), e70046. https://doi.org/10.1002/hyp.70046

Schooling, J.T. (2014). The influence of tree traits and storm event characteristics on stemflow production from isolated deciduous trees in an urban park. [Unpublished Master's Thesis] Retrieved from https://www.tru.ca/__shared/assets/Schooling_thesis34903.pdf

Schooling, J. T., & Carlyle-Moses, D. E. (2015). The influence of rainfall depth class and deciduous tree traits on stemflow production in an urban park. *Urban Ecosystems*, *18*(4), 1261–1284. https://doi.org/10.1007/s11252-015-0441-0

Schwärzel, K., Ebermann, S., & Schalling, N. (2012). Evidence of double-funneling effect of beech trees by visualization of flow pathways using dye tracer. *Journal of Hydrology*, *470–471*, 184–192. https://doi.org/10.1016/j.jhydrol.2012.08.048

Şensoy, H., & Tanyel, M. (2021). Effects of heavy rainfall on stemflow generation in some individual trees. *Fresenius Environmental Bulletin*, *30*, 7579–7595.

Siegert, C. M., & Levia, D. F. (2014). Seasonal and meteorological effects on differential stemflow funneling ratios for two deciduous tree species. *Journal of Hydrology*, *519*(PA), 446–454. https://doi.org/10.1016/j.jhydrol.2014.07.038

Silva, I. C., & Rodríguez, H. G. (2001). Interception loss, throughfall and stemflow chemistry in pine and oak forests in northeastern Mexico. *Tree Physiology*, *21*(12–13), 1009–1013. https://doi.org/10.1093/treephys/21.12-13.1009

Slatyer, R. O. (1965). Measurements of precipitation interception by an arid zone plant community (Acacia aneura F. Muell). Retrieved https://unesdoc.unesco.org/notice?id=p::usmarcdef_0000019997

Soulsby, C., Braun, H., Sprenger, M., Weiler, M., Tetzlaff, D., (2017). Influence of forest and shrub canopies on precipitation partitioning and isotopic signatures. *Hydrological Processes*. 31, 4282–4296. https://doi.org/10.1002/hyp.11351

Spencer, S. A., & van Meerveld, H. J. (2016). Double funnelling in a mature coastal British Columbia forest: Spatial patterns of stemflow after infiltration. *Hydrological Processes*, 30(22), 4185–4201. https://doi.org/10.1002/hyp.10936

Šraj, M., Brilly, M., Mikoš, M., 2008. Rainfall interception by two deciduous mediterranean forests of contrasting stature in Slovenia. *Agricultural and Forest Meteorology. 148*, 121–134. https://doi.org/10.1016/j.agrformet.2007.09.007.

Staelens, J., A. De Schrijver, and K. Verheyen (2007). Seasonal variation in throughfall and stemflow chemistry beneath a European beech (Fagus sylvatica) tree in relation to canopy phenology, *Canadian Journal of Forest Research, 37*(8), 1359–1372, https://doi.org/10.1139/X07-003

Staelens, J., de Schrijver, A., Verheyen, K., & Verhoest, N. E. C. (2008). Rainfall partitioning into throughfall, stemflow, and interception within a single beech (Fagus sylvatica L.) Canopy: influence of foliation, rain event characteristics, and meteorology. *Hydrological Processes*, *22*(1), 33–45. https://doi.org/10.1002/hyp.6610

Stewart, J. B. (1977). Evaporation from the wet canopy of a pine forest. *Water Resources Research*, *13*(6), 915–921. https://doi.org/10.1029/WR013i006p00915.

Su, L., Qi, L., Zhuang, W., & Zhang, Y. (2023). Contrasting effects of low-severity fire on stemflow production between coexisting pine and oak trees. *Science of The Total Environment, 858*, 159885. https://doi.org/10.1016/j.scitotenv.2022.159885

Tanaka, T., Taniguchi, M., & Tsujimura, M. (1996). Significance of stemflow in groundwater recharge. 2: A cylindrical infiltration model for evaluating the stemflow contribution to groundwater recharge. *Hydrological Processes*, *10*(1), 81–88. https://doi.org/10.1002/(SICI)1099-1085(199601)10:1<81::AID-HYP302>3.0.CO;2-M

Taniguchi, M., Tsujimura, M., & Tanaka, T. (1996). Significance of stemflow in groundwater recharge. 1: Evaluation of the stemflow contribution to recharge using a mass balance approach. *Hydrological Processes*, *10*(1), 71–80. https://doi.org/10.1002/(SICI)1099-1085(199601)10:1<71::AID-HYP301>3.0.CO;2-Q

Teklehaimanot, Z., Jarvis, P. G., & Ledger, D. C. (1991). Rainfall interception and boundary layer conductance in relation to tree spacing. *Journal of Hydrology*, *123*(3), 261–278. https://doi.org/10.1016/0022-1694(91)90094-X

Tischer, A., Michalzik, B., & Lotze, R. (2020). Nonuniform but highly preferential stemflow routing along bark surfaces and actual smaller infiltration areas than previously assumed: A case study on European beech (Fagus sylvatica L.) And sycamore maple (Acer pseudoplatanus L.). *Ecohydrology*, *13*(6). https://doi.org/10.1002/eco.2230

Tonello, K. C., Van Stan, J. T., Rosa, A. G., Balbinot, L., Pereira, L. C., & Bramorski, J. (2021). Stemflow variability across tree stem and canopy traits in the Brazilian Cerrado. *Agricultural and Forest Meteorology*, *308–309*, 108551. https://doi.org/10.1016/j.agrformet.2021.108551

Van Stan, J. T., & Gordon, D. A. (2018). Mini-Review: Stemflow as a resource limitation to near-stem soils. *Frontiers in Plant Science*, *9*. https://www.frontiersin.org/articles/10.3389/fpls.2018.00248

Van Stan, J. T., Jarvis, M. T., & Levia, D. F. (2010). An automated instrument for the measurement of bark microrelief. *Institute of Electrical and Electronics Engineers: Transactions on Instrumentation and Measurement*, *59*(2), 491–493. https://doi.org/10.1109/TIM.2009.2031338

Van Stan, J. T., & Levia, D. F. (2010). Inter- and intraspecific variation of stemflow production from Fagus grandifolia Ehrh. (American beech) and Liriodendron tulipifera L. (yellow poplar) in relation to bark microrelief in the eastern United States. *Ecohydrology*, *3*(1), 11–19. https://doi.org/10.1002/eco.83

Van Stan, J. T., & Pinos, J. (2024). Three fundamental challenges to the advancement of stemflow research and its integration into natural science. *Water (Switzerland)*, *16*(1). https://doi.org/10.3390/w16010117

Van Stan, J. T., Siegert, C. M., Levia, D. F., & Scheick, C. E. (2011). Effects of wind-driven rainfall on stemflow generation between codominant tree species with differing crown characteristics. *Agricultural and Forest Meteorology*, *151*(9), 1277–1286. https://doi.org/10.1016/j.agrformet.2011.05.008

Van Stan, J. T., Van Stan, J. H., & Levia, D. F. (2014). Meteorological influences on stemflow generation across diameter size classes of two morphologically distinct deciduous species. *International Journal of Biometeorology*, *58*(10), 2059–2069. https://doi.org/10.1007/s00484-014-0807-7

Wang, T., Hamann, A., Spittlehouse, D., & Aitken, S. (2006). Development of PRISM-based scale-free climate data for western Canada for use in resource management. *International Journal of Climatology*, *26*, 383–397. https://doi.org/10.1002/joc.1247

Wang, T., Hamann, A., Spittlehouse, D., & Murdock, T. (2012). ClimateWNA—High-resolution spatial climate data for western north america. *Journal of Applied Meteorology and Climatology*, *51*, 16–29. https://doi.org/10.1175/JAMC-D-11-043.1

Xiao, Q., E. G. McPherson, S. L. Ustin, M. E. Grismer, and J. R. Simpson (2000). Winter rainfall interception by two mature open-grown trees in Davis, California, *Hydrological Processes*, *14*(4), 763–784, https://doi.org/10.1002/(SICI)1099-1085(200003)14:4<763::AID-HYP971>3.0.CO;2-7

Yarranton, G. A. (1967). An instrument for measuring the microrelief of bark. *Canadian Journal of Botany*, *45*(8), 1173–1178. https://doi.org/10.1139/b67-125

Zabret, K., Rakovec, J., & Šraj, M. (2018). Influence of meteorological variables on rainfall partitioning for deciduous and coniferous tree species in urban area. *Journal of Hydrology*, *558*, 29–41. https://doi.org/10.1016/j.jhydrol.2018.01.025

Zabret, K., & Šraj, M. (2019). Rainfall interception by urban trees and their impact on potential surface runoff. *CLEAN – Soil, Air, Water*, *47*(8), 1800327. https://doi.org/10.1002/clen.201800327

Zabret, K., & Šraj, M. (2021). How characteristics of a rainfall event and the meteorological conditions determine the development of stemflow: A case study of a birch tree. *Frontiers in Forests and Global Change*, *4*. https://doi.org/10.3389/ffgc.2021.663100

Zhang, H., Fu, C., Liao, A., Zhang, C., Liu, J., Wang, N., & He, B. (2021). Exploring the stemflow dynamics and driving factors at both inter- and intra-event scales in a typical subtropical deciduous forest. *Hydrological Processes*, *35*(3), e14091. https://doi.org/10.1002/hyp.14091

Zhang, H., Levia, D. F., He, B., Wu, H., Liao, A., Carlyle-Moses, D. E., Liu, J., Wang, N., Li, J., & Fu, C. (2020). Interspecific variation in tree- and stand-scale stemflow funneling ratios in a subtropical deciduous forest in eastern China. *Journal of Hydrology*, *590*, 125455. https://doi.org/10.1016/j.jhydrol.2020.125455

Zhang, Y., Wang, X., Pan, Y., & Hu, R. (2021). How do rainfall intensity and raindrop size determine stemflow production? Quantitative evaluation from field rainfall simulation experiments. *Hydrological Sciences Journal*, *66*(13), 1979–1985. https://doi.org/10.1080/02626667.2021.1974024

Zhang, Y., Wang, X., Hu, R., Pan, Y., & Paradeloc, M. (2015). Rainfall partitioning into throughfall, stemflow and interception loss by two xerophytic shrubs within a rain-fed re-vegetated desert ecosystem, northwestern China. *Journal of Hydrology*, *527*, 1084–1095. https://doi.org/10.1016/j.jhydrol.2015.05.060

Zhao, X., Asawa, T., Kiyono, T., & Oshio, H. (2025). Quantifying the rainfall-partitioning process of an urban isolated tree during different rainfall events for stormwater management. *Urban Climate*, *59*, 102326. https://doi.org/https://doi.org/10.1016/j.uclim.2025.102326

Chapter 3: Conclusion and Recommendations for Future Study

3.1 Applicability to Current Literature

My study confirms the importance of S_F to ponderosa pine as a point-source input of water into the soil, especially in semi-arid environments where this species is often situated. While originally considered negligible due to the small percentage of precipitation it represents, a smattering of studies throughout the history of S_F study such as Reigler (1881), Rowe (1949) and Pressland (1976), have posited the importance of S_F. Within the last 35 years, researchers have better understood how important S_F can be to ecosystems (e.g., Návar and Bryan 1990; Taniguchi et al. 1996; Chang and Matzner 2000; Staelens et al. 2007; Návar 2011; Carlyle-Moses et al 2018; Llorens et al. 2022; Katul et al. 2025; Levia et al. 2025), and the assumption of stemflow being unimportant is now defunct. Trees in my study produced equivalent rainfall depths greater than anticipated and in excess of previous studies (e.g., McKee and Carlyle-Moses 2017, González-Martínez et al. 2022) despite low rainfall input. Like previous studies, high precipitation amounts resulted in greater S_F yields (e.g. Park and Cameron 2008, Schwärzel et al. 2012, Fan et al. 2015, Tonello et al. 2021). However, ponderosa pine also excels at delivering large amounts of water to its bole during high-intensity, low precipitation storms when branching angles are high. This is especially important in semi-arid areas, as their precipitation events tend to be high-intensity with low precipitation (Elkollaly and Sherif 2025). Since S_F is a concentrated input at the base of a tree or plant, it has implications for groundwater contribution and possible water permanently available for trees to take up during droughts. The high S_F efficiency and funneling ratios of ponderosa pine suggest that they will survive much more easily in drought-like conditions than other species (Mckee 2010, Gordon et al. 2020). However, to better understand the importance of S_F in semi-arid systems, it is important to expand the research to trees of different ages and different species, as not all will behave the same way (Snyder et al. 2024).

3.2 Limitations

Stemflow studies undertaken to date have several limitations that need to be addressed in future exploration into S_F generation and infiltration. Currently, there is a lack of consensus on simulation methodologies that would allow for direct comparison between studies (Llorens et al. 2022). Presently, there are two accepted methods for measuring S_F infiltration area. The first is applying dye directly to the base of the tree using standard methodologies and observing the movement of natural S_F down the stem into the soil (e.g. Carlyle-Moses et al. 2018; Gonzalez et al. 2020). The advantage of this method is that it permits observation without altering the tree's natural processes. However, a significant limitation is that the feasibility of quantifying Q_{SF} remains unclear even if long-term S_F monitoring is used to establish whether these relationships can be meaningfully quantified. This is due to the values of meteorological variables such as rainfall intensity and wind speed during monitoring being different to variables during simulation (Llorens et al. 2022). The second method involves applying dye to a collection bucket and using a perforated tube to evenly distribute simulated S_F around the tree trunk (e.g., Schwärzel et al. 2012; Llorens et al. 2022). An advantage of this approach is that Q_{SF} is controlled by the researcher, allowing other environmental conditions such as litter removal or soil saturation to be systematically modified. However, a key limitation of the approach is that in natural conditions, stemflow is rarely distributed uniformly around the trunk due to variations in tree morphology and meteorological conditions (Tischer et al. 2020). Therefore, the resulting infiltration patterns may not accurately represent natural conditions. Comparable methods are needed so that any differences in S_F infiltration measurements can be attributed solely to differences in tree species, morphology, and soil characteristics rather than to methodologies.

Similar to other studies (e.g. Schwärzel et al., 2012; Llorens et al. 2022), when I measured I_t, I removed the litter around my trees to better observe the dyed soil. The issue with removing litter is that S_F may travel farther along certain litter, such as pine needles, leaves, or bark, than without litter. Conversely, the litter may also prevent water from spreading further (e.g., Walsh & Voigt, 1977; Dunkerley, 2015). A possible solution may lie in the methodology used by Pinos et al. (2023) who carefully removed the litter after the simulation was finished in order to measure infiltration area. It may be prudent for future

research to study both littered and non-littered conditions on similarly sized trees on similar topography to observe how they differ in *It*.

3.2 Future Research

While my study has comprehensively investigated how ponderosa pine S_F generation is affected by meteorological and tree morphological variables, there remains a significant knowledge gap regarding how society can use such stemflow research to understand the linkages between natural and artificial water processes. This decade (2023-2032), the International Association of Hydrological Sciences is enacting the HELPING initiative. HELPING is an acronym standing for Hydrology Engaging Local People IN one Global World. In the spirit of contributing to this initiative, the study of S_F must evolve to address its unresolved issues and expand its relevance across disciplines. Building on the challenges and questions discussed by previous researchers (e.g. Van Stan and Allen 2020; Metzger et al. 2021; Su et al. 2023; Van Stan and Pinos 2024; Katul et al. 2025; Levia et al. 2025) the following should provide a guide for future studies.

Within the idea of bringing hydrologic and therefore S_F research to everyday issues, there is a need to assess the context-specific impacts S_F has upon urban systems, agriculture, and forests. A couple of recent studies were conducted upon how S_F could be repurposed from runoff to become a supplemental source of irrigation for green infrastructure (Antoine et al. 2025; Levia et al. 2025). However, more studies need to be conducted over a range of conditions to identify S_F as a reliable stormwater management and agricultural recharge option (Carlyle-Moses and Schooling 2015). In addition, there is a need for the evaluation of the contribution of S_F to crop water use efficiency and soil salinity in irrigated vs. rainfed systems. While the majority of S_F research has been conducted upon trees, there are some more recent studies that have focused upon crops (e.g. Guo et al. 2022; Guo et al. 2026). However, as noted in Antoneli et al (2021), the majority of research has been conducted in the northern hemisphere. Therefore, more studies need to be conducted south of the equator. Lastly, as the effects of climate change become increasingly important, there is a need to link S_F variability to tree drought resilience, wildfire risk, and species competition. While there have been some studies that have looked at how wildfires affect S_F (e.g. Su et al. 2023), there are none describing the mitigating effect S_F may have on potential wildfires. In addition,

research has begun on how S_F may affect a tree's ability to resist a warming climate, and how a warming climate may affect S_F itself (e.g. Levia 2003; Levia and Germer 2015; Antoine et al. 2025) however more are needed.

As the human species continues be the primary driver of changes to the natural world, it is important to understand how those changes affect processes such as S_F distribution. There is a growing body of research upon canopy interactions with atmospheric deposition, suggesting that trees can provide direct pathways for both helpful and harmful particulate matter (Van Stan et al. 2021). Vegetation canopies are interception surfaces for airborne particulate matter, functioning as environmental filters that accumulate atmospheric contaminants over time (Weber & Bigalke. 2025). Conceptual studies further demonstrate that foliar surfaces can retain microplastics and other particulates, which may subsequently be mobilised by precipitation events (e.g. Li et al. 2025). While S_F study is not yet included in research on tree interception of microplastics, it is likely that it contributes greatly to particulate deposition into soil. This assumption is based upon the point-source nutrient infiltration of S_F, which strongly suggests that stemflow may represent an underexplored and potentially significant pathway for microplastic transport in forested and urban environments.

Future research should investigate the potential of S_F chemistry as indicators of canopy processes and as functional components of engineered ecosystems. Sugars detected in S_F are likely products of apoplastic exchange and bark leaching rather than direct measures of internal phloem metabolism (Levia et al. 2025). However their concentrations may provide insight into broader physiological responses related to carbon allocation, environmental stress, and seasonal acclimation (Levia et al. 2024; Levia et al. 2025). Integrating stemflow hydrology with plant physiology and solute transport studies could therefore establish stemflow as a non-destructive tool for monitoring tree function and ecosystem health. Furthermore, incorporating stemflow chemistry into hydrological and green infrastructure models may improve predictions of localized carbon and nutrient inputs to urban soils (Antoine et al. 2025). Therefore, the design of tree-based green infrastructure systems may be needed simultaneously manage excess water and enhance ecosystem health withing urban areas.

Tree species differ substantially in S_F production, and certain soil characteristics strongly influence saturated hydraulic conductivity (K_{sat}). Therefore, species-specific research is warranted. In my study, I did not examine the fate of stemflow following infiltration; therefore, future research on ponderosa pine should specifically focus on determining how S_F infiltration and subsurface redistribution compare with those of other species. Additionally, experimental work conducted at a similar site that replicates the range of K_{sat} values observed in this study may help to clarify how ponderosa influences S_F movement and storage. For congruency, researchers may consider using trees of similar size and morphology to those within my study. For further inquiry, one may consider expanding the scope of research to include a wider range of morphologies and sizes. There are several methodologies, both invasive and non-invasive, that have been developed to study how trees funnel S_F belowground. As with S_F simulations, there are two most commonly accepted practices: using soil moisture sensors to monitor changes in underground water (e.g., Liang et al. (2011) and using dye tracers to trace preferential flow paths through the soil (Pinos et al. 2023). However, both methods have a weakness in that they disrupt natural soil and water cycle processes. In order to combat this, more recently ground penetrating radar has been used (Guo et al. 2020; di Prima et al 2023).

It is still largely unknown where S_F goes after infiltrating into the soil surface. Through the use of technologies such as isotopic tracers, dye experiments, and ground penetrating radar, we may be able to follow S_F's underground paths for some distance (e.g. Guo et al. 2020; Di Prima et al. 2023) In addition, once S_F infiltrates, there is a need to investigate its role in nutrient cycling, microbial activity, and plant-microbe symbioses, especially in nutrient-poor soils. This also leads to a need for the development of a method to assess how S_F sustains niche ecosystems. Some studies have focused upon how epiphytes affect S_F and vice versa (e.g. Pypker et al. 2006; Pryet et al 2012; Chen et al. 2019), however there is a lack of research on how S_F affects soil-based ecosystems. While there are some studies emerging on the topic (e.g. Metzger et al. 2021; Teachey et al. 2022), further research is needed to see whether the effect is similar or different across species.

While bringing future S_F research in line with the goals of IAHS is important, in order to do so, researchers need to address several limitations of the field. There are several

important gaps in the current understanding of S_F hydrodynamics, emphasizing the need to move towards a more mechanistic understanding of water movement along the stem. Katul et al. (2025) provide a guide for future researchers, should they choose to investigate this further. As evidenced in my study, there are several different types of flow water becomes as it travels towards the soil. There are generally three types of flow, sheet flow, rivulets, and droplets (Katul et al. 2025). On ponderosa pine trees, I observed both rivulets and droplet flow, depending on whether the S_F pathed between thick bark pieces or upon them. In some cases, droplets left the tree only to land on a lower part of the tree (See videos in Appendix B). This kind of bark routing is understudied in S_F research and may be more accurately represented as networks of preferential flow rather than uniform flow surfaces (see Katul et al. 2025). Most stemflow studies measure only the total volume of water collected at the base of a tree. While this provides information on how much stemflow occurs, it reveals little about how water moved down the stem. Therefore, Katul et al. (2025) propose high-resolution observations capable of resolving centimetre- to millimetre-scale flow patterns and second-scale changes in flow behaviour are therefore needed to identify the mechanisms governing stemflow routing. In addition, much of the current research assumes that S_F acts as pure water with constant physical properties. Due to the solutes picked up by the tree, such as microplastics, nutrients, and surfactants, the water may be altered to the point where it no longer flows like pure water. While there are no studies researching this interaction with regards to S_F, Katul et al. (2025) stress that it needs exploration.

Researchers need to develop methods to map the specific canopy zones that generate S_F. Some researchers such as Van stan and Pinos (2024) have posited that not all areas of a canopy generate S_F or generate it efficiently, so more precise methodologies for measuring S_F generation within specific areas of the canopy should be implemented. In addition, the S_F variability intra- and interspecies must be investigated to study individual trees. The inconsistency in variables on S_F production and lack of understanding of its drivers and patterns limit accurate global-scale predictions under changing climate conditions, thus researchers will need to develop advanced methods using existing technologies (e.g., LiDAR, hyperspectral imaging, IoT sensors) to map the specific canopy zones generating S_F, and further quantify how bark texture, branching architecture, size, and leaf traits funnel water to stems.

There are several potential sources of S_F that are underrepresented in the literature; there is a need for holistic monitoring across conditions. There are only three known studies looking at condensation (Ney 1893; Shure and Lewis 1973; Gordon et al. 2020), three looking at S_F generated by snowmelt (Rowe and Hendrix 1951; Miller, 1966; Herwitz and Levia 1997), and one using mixed rain/snow precipitation (Levia 2004). Due to the limited number of studies as well as a lack of modern research, I believe it is prudent for future researchers to examine this area of S_F science.

Additional S_F research is needed on ponderosa pine trees. There are only three studies that mention S_F on ponderosa pine trees (Johnson 1942; Rowe and Hendrix 1951; Orr 1972), as a result, limited data and information is available on the effects ponderosa have on S_F chemistry, such as the delivery of nitrogen, carbon, and phosphorus to the soil. S_F chemistry has been studied on other species however (e.g. Herwitz 1991; Kuraji et al. 2001; Wu et al. 2024), providing future researchers with a methodology that can be used when studying ponderosa pine. Questions need to be answered, such as: when does the plant use these nutrients? How long does the deeply infiltrated water remain available for plant uptake? Since organic matter is often higher closer to a tree's stem, does S_F contribute to organic matter deposition, or is most matter just falling off the tree? What effect does S_F have on the groundwater table? Delving into these questions will allow us to better understand how ponderosa S_F interacts with its surrounding environment and whether it is, a significant contributor to tree survival in drought-like conditions. As S_F is usually spatially concentrated at the base of the tree trunk, tree roots may provide a direct conduit to the groundwater table, especially in taproot species such as ponderosa pine (e.g., Johnson and Lehmann 2006; Pinos et al. 2023). S_F's ability to infiltrate deeply into the soil is influenced by interactions among many factors. The variety, quantity, and intercorrelations of these components are topics for further inquiry. This was an area in my study that I wished to explore further, however the amount of work involved would be outside the scope of a master's degree. As such, a comprehensive study of S_F infiltration/saturated hydraulic conductivity and how it is connected to soil characteristics needs to be conducted upon ponderosa-generated S_F.

Future researchers may foster partnerships between hydrologists, ecologists, soil scientists, and climate modelers to build unified frameworks for S_F study. Perhaps there is

room to incorporate Indigenous knowledge and citizen science to document S_F's cultural and ecological roles in traditional landscapes. The goal of S_F study is for policymakers and forest harvesters to understand which trees/plants are more necessary to ecosystem health in the context of S_F than others. Researchers need to translate their study findings into actionable guidelines for sustainable forestry, urban planning, and water resource management. By bridging gaps in observation, theory, and application, S_F research can transition from a niche curiosity to a cornerstone of holistic environmental science—equipping society to better manage water, biodiversity, and climate challenges in an era of global change.

3.4 References

Antoine, J., Lin, M., El-Kulak, A. M., & van Stan, J. T. (2025). Tapping the urban forest: Integrating tree canopy runoff (stemflow) into blue-green infrastructure. *Urban Forestry & Urban Greening*, *111*, 128876. https://doi.org/10.1016/j.ufug.2025.128876

Antoneli, V., de Jesus, F. C., Bednarz, J. A., & Thomaz, E. L. (2021). Stemflow and throughfall in agricultural crops: A synthesis. *Revista Ambiente & Água*, *16*(1), 1–11. https://doi.org/10.4136/ambi-agua.2528

Carlyle-Moses, D. E., Iida, S., Germer, S., Llorens, P., Michalzik, B., Nanko, K., Tischer, A., & Levia, D. F. (2018). Expressing stemflow commensurate with its ecohydrological importance. *Advances in Water Resources*, *121*, 472–479. https://doi.org/10.1016/j.advwatres.2018.08.015

Carlyle-Moses, D. E., & Schooling, J. T. (2015). Tree traits and meteorological factors influencing the initiation and rate of stemflow from isolated deciduous trees. *Hydrological Processes*, *29*(18), 4083–4099. https://doi.org/10.1002/hyp.10519

Chang, S.-C., & Matzner, E. (2000). The effect of beech stemflow on spatial patterns of soil solution chemistry and seepage fluxes in a mixed beech/oak stand. *Hydrological Processes*, *14*(1), 135–144. https://doi.org/10.1002/(SICI)1099-1085(200001)14:1<135::AID-HYP915>3.0.CO;2-R

Chen, L.-C., Wang, L.-J., Martin, C. E., & Lin, T.-C. (2019). Mediation of stemflow water and nutrient availabilities by epiphytes growing above other epiphytes in a subtropical forest. *Ecohydrology*, *12*(7), e2140. https://doi.org/10.1002/eco.2140

di Prima, S., Fernandes, G., Marras, E., Giadrossich, F., Stewart, R. D., Abou Najm, M. R., Winiarski, T., Mourier, B., Angulo-Jaramillo, R., Comegna, A., del Campo, A., & Lassabatere, L. (2023). Evaluating subsurface flow connectivity in a pine-covered hillslope with stemflow infiltration and ground-penetrating radar surveys. *Journal of Hydrology*, *620*, 129527. https://doi.org/10.1016/j.jhydrol.2023.129527

Dunkerley, D. (2015). Percolation through leaf litter: What happens during rainfall events of varying intensity? *Journal of Hydrology*, *525*, 737–746. https://doi.org/10.1016/J.JHYDROL.2015.04.039

Elkollaly, M., & Sherif, M. (2025). Event-based rainfall dynamics and storm frequency in arid and semi-arid climates: an innovative standardized approach for rainstorm analysis. *Journal of Hydrology*, *659*, 133231. https://doi.org/10.1016/j.jhydrol.2025.133231

Fan, J., Oestergaard, K. T., Guyot, A., Jensen, D. G., & Lockington, D. A. (2015). Spatial variability of throughfall and stemflow in an exotic pine plantation of subtropical coastal Australia. *Hydrological Processes*, *29*(5), 793–804. https://doi.org/10.1002/hyp.10193

Gonzalez-Ollauri, A., Stokes, A., & Mickovski, S. B. (2020). A novel framework to study the effect of tree architectural traits on stemflow yield and its consequences for soil-water dynamics. *Journal of Hydrology*, *582*. https://doi.org/10.1016/j.jhydrol.2019.124448

González-Martínez, T. M., Williams-Linera, G., & Holwerda, F. (2022). Interactive effects of functional traits and rainfall event size on stemflow in a tropical montane cloud forest. *Ecohydrology*, *15*(8), e2466. https://doi.org/10.1002/eco.2466

Gordon, D. A. R., Coenders-Gerrits, M., Sellers, B. A., Sadeghi, S. M. M., & van Stan II, J. T. (2020). Rainfall interception and redistribution by a common north american understory and pasture forb, eupatorium capillifolium (lam. Dogfennel). *Hydrology and Earth System Sciences*, *24*(9), 4587–4599. https://doi.org/10.5194/hess-24-4587-2020

Guo, M., He, J., Dong, K., Yang, N., Li, Y., Xiao, J., & Feng, L. (2022). Factors influencing maize (zea mays) stemflow in western Liaoning, China. *Agronomy Journal*. https://doi.org/10.1002/agj2.21234

Guo, L., Mount, G. J., Hudson, S., Lin, H., & Levia, D. (2020). Pairing geophysical techniques improves understanding of the near-surface critical zone: visualization of preferential routing of stemflow along coarse roots. *Geoderma*, *357*, 113953. https://doi.org/10.1016/j.geoderma.2019.113953

Guo, B., Yang, H., Zhu, C. Y., Yan, Z. B., Cao, J. S., & Shen, Y. J. (2026). Rainfall partitioning and interception simulation for typical species in the Taihang Mountains, China. *Agricultural And Forest Meteorology*, *378*. https://doi.org/10.1016/j.agrformet.2025.111004

Hamilton, & E. L. Rowe, P. B., (1949). Rainfall interception by chaparral in California. State of California, Dept. of Natural Resources, Division of Forestry. https://catalog.hathitrust.org/Record/009110632

Herwitz, S. R. (1991). Aboveground adventitious roots and stemflow chemistry of Ceratopetalum virchowii in an Australian montane tropical rain forest. *Biotropica*, *23*(3), 210–218. https://doi.org/10.2307/2388197

Herwitz, S. R., & Levia Jr., D. F. (1997). Mid-winter stemflow drainage from bigtooth aspen (Populus grandidentata Michx.) in central Massachusetts. *Hydrological Processes*, *11*(2), 169–175. https://doi.org/10.1002/(SICI)1099-1085(199702)11:2<169::AID-HYP428>3.0.CO;2-J

Johnson, M. S., & Lehmann, J. (2006). Double-funneling of trees: Stemflow and root-induced preferential flow. *Écoscience*, *13*(3), 324–333. https://doi.org/10.2980/i1195-6860-13-3-324.1

Johnson, W. M. (1942). The interception of rain and snow by a forest of young ponderosa-pine. *Eos, Transactions American Geophysical Union*, *23*(2), 566–570. https://doi.org/10.1029/TR023i002p00566

Katul, G. G., Keshavarz, B., Meydani, A., & Levia, D. F. (2025). Stemflow hydrodynamics. *Reviews of Geophysics*, *63*(3), e2024RG000857. https://doi.org/10.1029/2024RG000857

Kuraji, K., Tanaka, Y., Tanaka, N., & Karakama, I. (2001). Generation of stemflow volume and chemistry in a mature japanese cypress forest. *Hydrological Processes*, *15*(10), 1967–1978. https://doi.org/10.1002/hyp.250

Levia, D. F., & Frost, E. E. (2003). A review and evaluation of stemflow literature in the hydrologic and biogeochemical cycles of forested and agricultural ecosystems. *Journal of Hydrology*, *274*(1), 1–29. https://doi.org/10.1016/S0022-1694(02)00399-2

Levia, D. F., & Germer, S. (2015). A review of stemflow generation dynamics and stemflow-environment interactions in forests and shrublands. In *Reviews of Geophysics, 53*(3), 673–714. Blackwell Publishing Ltd. https://doi.org/10.1002/2015RG000479

Levia, D. F., Katul, G. G., Meydani, A., Nanko, K., Yuan, C., Zhang, Y., Llorens, P., & Bruen, M. (2025). Towards smarter green infrastructure: fusing bark ecology and stemflow hydrodynamics on tree stems. *Ecological Indicators*, *178*, 113827. https://doi.org/10.1016/j.ecolind.2025.113827

Levia, D. F., O'Halloran, R. C., Otsuka, Y., Chang, J. L., Kaiser, K., Nanko, K., Iida, S., Shapiro, A. J., Gupta, Y., Sadula, S., Vlachos, D. G., & Epps III, T. H. (2025). Stemflow Unveils Trees' Weatherproofing Stratagem During Autumnal Senescence. *Plant, Cell & Environment*, *48*(9), 7001–7004. https://doi.org/10.1111/pce.15668

Levia, D. F., O'Halloran, R. C., Otsuka, Y., Chang, J., Kaiser, K., Nanko, K., Iida, S., Shapiro, A., Gupta, Y., Sadula, S., Vlachos, D. G., & Epps III, T. H. (2024). Stemflow neutral sugar concentrations and the physiological ecology of trees: new data and a new perspective. *AGU Fall Meeting Abstracts, AGU Fall Meeting Abstracts*, *2024*, H41C-01.

Li, Y., Zhang, J., Xu, L., Li, R., Zhang, R., Li, M., Ran, C., Rao, Z., Wei, X., Chen, M., Wang, L., Li, Z., Xue, Y., Peng, C., Liu, C., Sun, H., Xing, B., & Wang, L. (2025). Leaf absorption contributes to accumulation of microplastics in plants. *Nature*, *641*(8063), 666–673. https://doi.org/10.1038/s41586-025-08831-4

Liang, W.-L., Kosugi, K., & Mizuyama, T. (2011). Soil water dynamics around a tree on a hillslope with or without rainwater supplied by stemflow. *Water Resources Research*, *47*(2). https://doi.org/10.1029/2010WR009856

Llorens, P., Latron, J., Carlyle-Moses, D. E., Näthe, K., Chang, J. L., Nanko, K., Iida, S., & Levia, D. F. (2022). Stemflow infiltration areas into forest soils around American beech (Fagus grandifolia Ehrh.) Trees. *Ecohydrology*, *15*(2). https://doi.org/10.1002/eco.2369

McKee, A. J. (2010). The quantitative importance of stemflow: An evaluation of past research and results from a study in Lodgepole Pine (Pinus contorta var. latifolia) stands in

Southern British Columbia. MSc thesis, Thompson Rivers University, Kamloops, British Columbia Canada. 113 p https://arcabc.ca/islandora/object/tru%3A28

McKee, A. J., & Carlyle-Moses, D. E. (2017). Modelling stemflow production by juvenile lodgepole pine (Pinus contorta var. Latifolia) trees. *Journal of Forestry Research*, *28*(3), 565–576. https://doi.org/10.1007/s11676-016-0336-9

Metzger, J. C., Filipzik, J., Michalzik, B., & Hildebrandt, A. (2021). Stemflow infiltration hotspots create soil microsites near tree stems in an unmanaged mixed beech forest. *Frontiers in Forests and Global Change*, *4*. https://doi.org/10.3389/ffgc.2021.701293

Miller, D. H. (1966). *Transport of intercepted snow from trees during snow storms (Vol. 33)*. Pacific Southwest Forest and Range Experiment Station, Forest Service, US Department of Agriculture. https://research.fs.usda.gov/treesearch/30643

Návar, J. (2011). Stemflow variation in Mexico's northeastern forest communities: Its contribution to soil moisture content and aquifer recharge. *Journal of Hydrology*, *408*(1–2), 35–42. https://doi.org/10.1016/j.jhydrol.2011.07.006

Návar, J., & Bryan, R. (1990). Interception loss and rainfall redistribution by three semi-arid growing shrubs in northeastern Mexico. *Journal of Hydrology*, *115*(1–4), 51–63. https://doi.org/10.1016/0022-1694(90)90197-6

Ney, C. E. (1893). *Der Wald und Quellen*. Franz Pietzcker. https://cir.nii.ac.jp/crid/1130282270940565248.bib?lang=en

Orr, H. K. (1972*). Throughfall and stemflow relationships in second-growth ponderosa pine in the Black Hills (Vol. 210)*. Rocky Mountain Forest and Range Experiment Station, Forest Service, US Department of Agriculture. https://books.google.ca/books?id=nJ_wiNy68v4C

Park, A., & Cameron, J. L. (2008). The influence of canopy traits on throughfall and stemflow in five tropical trees growing in a Panamanian plantation. *Forest Ecology and Management*, *255*(5–6), 1915–1925. https://doi.org/10.1016/j.foreco.2007.12.025

Pinos, J., Flury, M., Latron, J., & Llorens, P. (2023). Routing stemflow water through the soil via preferential flow: A dual-labelling approach with artificial tracers. *Hydrology and Earth System Sciences*, *27*(15), 2865–2881. https://doi.org/10.5194/hess-27-2865-2023

Pryet, A., Domínguez, C., Tomai, P. F., Chaumont, C., d'Ozouville, N., Villacís, M., & Violette, S. (2012). Quantification of cloud water interception along the windward slope of Santa Cruz Island, Galapagos (Ecuador). *Agricultural and Forest Meteorology*, *161*, 94–106. https://doi.org/10.1016/j.agrformet.2012.03.018

Pypker, T. G., Unsworth, M. H., & Bond, B. J. (2006). The role of epiphytes in rainfall interception by forests in the Pacific Northwest. II. Field measurements at the branch and

canopy scale. *Canadian Journal of Forest Research*, *36*(4), 819–832. https://doi.org/10.1139/x05-286

Riegler W. (1881). Beobachtungen über die Abfuhr meteorischen Wassers entlang den Hochstämmen. *Mitteil. Forstl. Bundes Versuchsanstalt Wien* 2, 234–246 Hamilton

Rowe, P. B., & T. M. Hendrix. (1951). Interception of rain and snow by second-growth ponderosa pine. *Eos, Transactions American Geophysical Union*, *32*(6), 903–908. https://doi.org/10.1029/TR032i006p00903

Pressland, A. J. (1976). Soil Moisture Redistribution as affected by Throughfall and Stemflow in an Arid Zone Shrub Community. In *Austrailian Journal of Botany* (Vol. 24). https://doi.org/10.1071/BT9760641

Schooling, J. T., & Carlyle-Moses, D. E. (2015). The influence of rainfall depth class and deciduous tree traits on stemflow production in an urban park. *Urban Ecosystems*, *18*(4), 1261–1284. https://doi.org/10.1007/s11252-015-0441-0

Schwärzel, K., Ebermann, S., & Schalling, N. (2012). Evidence of double-funneling effect of beech trees by visualization of flow pathways using dye tracer. *Journal of Hydrology*, *470–471*, 184–192. https://doi.org/10.1016/j.jhydrol.2012.08.048

Snyder, K. A., Morrow, A. C., Stringham, T. K., & Allen, S. T. (2024). Do trees use stemflow water? A manipulative experiment on Singleleaf piñon and Utah juniper in Great Basin woodlands. *Tree Physiology*, *44*(12), tpae143. https://doi.org/10.1093/treephys/tpae143

Shure, D. J., & Lewis, A. J. (1973). Dew formation and stem flow on common ragweed (Ambrosia artemisiifolia). *Ecology*, *54*(5), 1152–1155. https://doi.org/10.2307/1935583
Staelens, J., de Schrijver, A., & Verheyen, K. (2007). Seasonal variation in throughfall and stemflow chemistry beneath a European beech (Fagus sylvatica) tree in relation to canopy phenology. *Canadian Journal of Forest Research*, *37*(8), 1359–1372. https://doi.org/10.1139/X07-003

Staelens, J., de Schrijver, A., Verheyen, K., & Verhoest, N. E. C. (2008). Rainfall partitioning into throughfall, stemflow, and interception within a single beech (Fagus sylvatica L.) canopy: influence of foliation, rain event characteristics, and meteorology. *Hydrological Processes*, *22*(1), 33–45. https://doi.org/10.1002/hyp.6610

Su, L., Qi, L., Zhuang, W., & Zhang, Y. (2023). Contrasting effects of low-severity fire on stemflow production between coexisting pine and oak trees. *Science of The Total Environment*, *858*, 159885. https://doi.org/10.1016/j.scitotenv.2022.159885

Taniguchi, M., Tsujimura, M., & Tanaka, T. (1996). Significance of stemflow in groundwater recharge. 1: Evaluation of the stemflow contribution to recharge using a mass balance approach. *Hydrological Processes*, *10*(1), 71–80. https://doi.org/10.1002/(SICI)1099-1085(199601)10:1<71::AID-HYP301>3.0.CO;2-Q

Teachey, M. E., Ottesen, E. A., Pound, P., & van Stan II, J. T. (2022). Under the canopy: disentangling the role of stemflow in shaping spatial patterns of soil microbial community structure underneath trees. *Environmental Microbiology*, *24*(9), 4001–4012. https://doi.org/10.1111/1462-2920.15970

Tischer, A., Michalzik, B., & Lotze, R. (2020). Nonuniform but highly preferential stemflow routing along bark surfaces and actual smaller infiltration areas than previously assumed: A case study on European beech (Fagus sylvatica L.) and sycamore maple (Acer pseudoplatanus L.). *Ecohydrology*, *13*(6). https://doi.org/10.1002/eco.2230

Tonello, K. C., van Stan, J. T., Rosa, A. G., Balbinot, L., Pereira, L. C., & Bramorski, J. (2021). Stemflow variability across tree stem and canopy traits in the Brazilian Cerrado. *Agricultural and Forest Meteorology*, *308–309*, 108551. https://doi.org/10.1016/j.agrformet.2021.108551

Van Stan, J. T., & Allen, S. T. (2020). What We Know About Stemflow's Infiltration Area. *Frontiers in Forests and Global Change*, *3*. https://doi.org/10.3389/ffgc.2020.00061

Van Stan, J. T., & Pinos, J. (2024). Three Fundamental Challenges to the Advancement of Stemflow Research and Its Integration into Natural Science. *Water (Switzerland)*, *16*(1). https://doi.org/10.3390/w16010117

van Stan II, J. T., Ponette-González, A. G., Swanson, T., & Weathers, K. C. (2021). Throughfall and stemflow are major hydrologic highways for particulate traffic through tree canopies. *Frontiers in Ecology and the Environment*, *19*(7), 404–410. https://doi.org/10.1002/fee.2360

Walsh, R. P. D., & Voigt, P. J. (1977). Vegetation Litter: An Underestimated Variable in Hydrology and Geomorphology. *Journal of Biogeography*, *4*(3), 253–274. https://doi.org/10.2307/3038060

Weber, C. J., & Bigalke, M. (2025). Forest soils accumulate microplastics through atmospheric deposition. *Communications Earth & Environment*, *6*(1), 702. https://doi.org/10.1038/s43247-025-02712-4

Wu, M.-D., Jiang, Z.-Y., Yang, X., Yeerbolati, B., Huang, L., Zhong, Y.-Y., Zhang, H.-W., & Li, X.-Y. (2024). Global quantitative synthesis on the patterns and drivers of funneling ratio and enrichment ratio for stemflow. *CATENA*, *244*, 108253. https://doi.org/10.1016/j.catena.2024.108253

Appendix A: Recommendations or Future Research in Similar Forest Stands

Stemflow Collection Containers:

This study was conducted on ponderosa pine (*Pinus ponderosa*) in a semi-arid environment. Because coniferous species typically generate lower S_F volumes than deciduous species, a 19 L collection container was initially selected and was generally sufficient to capture event-scale S_F without approaching capacity. However, during a storm event delivering 23 mm of precipitation, Tree J produced 17.3 L of S_F, bringing the container close to overflow and risking data loss. Based on this observation, we recommend that future studies employ collection reservoirs with greater capacity than initially anticipated to reduce the likelihood of overflow during high-intensity or anomalous precipitation events.

Wildlife Deterrents:

The study site was in semi-urban parkland within municipal boundaries that retained natural habitat characteristics. Consequently, the area was frequented by deer and small mammals. Collection containers were fitted with lids to limit wildlife interference (e.g., drinking or bathing) and to reduce evaporative losses. Over the field season, numerous containers were also occupied by black widow spiders (*Latrodectus* spp.). For studies conducted in regions where unwanted creatures are present, I recommend installing fine mesh over container openings to protect them. Researchers should also assess local wildlife hazards and implement appropriate safety precautions prior to and during field deployment.

Human Interaction:

The study area was situated within a popular outdoor recreation site that received regular visitation. Members of the public frequently approached field personnel with questions regarding the research, which increased time demands during data collection. Future researchers working in publicly accessible areas should anticipate public interest and consider providing informational signage or an accessible website to communicate study objectives and methods, thereby reducing interruptions to field activities while still supporting public engagement.

Anchor Materials:

To reduce overturning under high wind conditions and minimize evaporative loss, collection containers were buried approximately 38 cm below ground surface. Graduated cylinders and tipping-bucket rain gauges were secured using wooden stakes and zip ties. Although these measures prevented complete toppling, strong winds occasionally displaced gauges from vertical alignment. Additional stabilization of gauges—such as securing them to metal poles or using more robust anchoring systems—is recommended to maintain proper alignment and measurement accuracy under high-wind conditions. Burying collection reservoirs below ground level proved effective limiting evaporation and maintaining container stability and is recommended for similar environments

Evaporation:

An issue with S_F research in more arid environments, as I confirmed in my study, is the rapid evaporation of S_F from collection containers, leading to a constant need for researchers to measure S_F levels immediately after a precipitation event. Therefore, the design of robust, automated sensors capable of capturing high-resolution, real-time S_F dynamics across diverse climates (e.g., arid zones, boreal winters) may be a viable solution for researchers seeking to simplify the logistics of their studies. A possible avenue may be to utilize HOBO data loggers connected to leaf wetness sensors affixed to the end of S_F collection tubes. This was an avenue I explored during the beginning stages of my study; however, I lacked the necessary equipment to implement it.

Appendix B: Images Throughout the Study

Figure B.1. Stemflow simulation apparatus (Sept. 2022).

Figure B.2. Tree M-4’s stemflow collection apparatus (Sep. 2022).

Figure B.3. Images captured of drip in midair (Oct. 2022).

Video Documentation of Simulated Stemflow

https://www.youtube.com/playlist?list=PLsm6BKDd8MRfOt3ZwgLyc8w6qxgm5w3rh

Figure B.4. Stem-angle measurement of Tree M-7 (Sep. 2021)